Gut dysbiosis contributes to the imbalance of Treg and Th17 cells in Graves' disease patients by propionic acid

Xinhuan Su[1,2,3], Xianlun Yin[2], Yue Liu[1,2,3], Xuefang Yan[2], Shucui Zhang[2], Xiaowei Wang[2], Zongwei Lin[2], Xiaoming Zhou[1], Jing Gao[2], Zhe Wang[1,3*], Qunye Zhang[2*]

[1] Department of Endocrinology, Shandong Provincial Hospital, Cheeloo College of Medicine, Shandong University, Shandong Provincial Key Laboratory of Endocrinology and Lipid Metabolism, Institute of Endocrinology and Metabolism, Shandong Academy of Clinical Medicine, Jinan, Shandong, 250021, China

[2] Key Laboratory of Cardiovascular Remodeling and Function Research, Chinese Ministry of Education, Chinese National Health Commission and Chinese Academy of Medical Sciences; State and Shandong Province Joint Key Laboratory of Translational Cardiovascular Medicine; Department of Cardiology, Qilu Hospital, Cheeloo College of Medicine, Shandong University, Jinan, 250012, China

[3] Division of Geriatrics, Shandong Provincial Hospital, Cheeloo College of Medicine, Shandong University, Jinan, 250021, China

* corresponding authors

Contact details:

Xinhuan Su: 1165998087@qq.com

Xianlun Yin: yinxianlun@163.com

Yue Liu: 909315593@qq.com

Xuefang Yan: 846028763@qq.com

Shucui Zhang: 576113937@qq.com

Xiaowei Wang: wxw11130@163.com

Zongwei Lin: fancy-achieve2008@163.com

Xiaoming Zhou: sdslyy@yeah.net

Jing Gao: 1126167719@qq.com

Zhe Wang: 18615206628@163.com

Qunye Zhang: wz.zhangqy@sdu.edu.cn

Corresponding Author

Zhe Wang,

Department of Endocrinology, Shandong Provincial Hospital, Cheeloo College of Medicine, Shandong University, Shandong Provincial Key Laboratory of Endocrinology and Lipid Metabolism, Institute of Endocrinology and Metabolism, Shandong Academy of Clinical Medicine, Jing 5 Wei 7 Road 324#, Jinan, Shandong Province, 250021, China.

Email 18615206628@163.com

Qunye Zhang,

Key Laboratory of Cardiovascular Remodeling and Function Research, Chinese Ministry of Education, Chinese National Health Commission and Chinese Academy of Medical Sciences; State and Shandong Province Joint Key Laboratory of Translational Cardiovascular

Medicine; Department of Cardiology, Qilu Hospital, Cheeloo College of Medicine, Shandong University, Wenhua Xi Road 107#, Jinan, Shandong Province, 250012, China.

Email wz.zhangqy@sdu.edu.cn

Funding

This work was supported by the National Natural Science Foundation of China (NO. 81570712 and 81670247) and the Natural Science Outstanding Youth Foundation of Shandong Province (NO. JQ201519), Major Science and Technology Innovation Project of Shandong Province (NO. 2018CXGC1218) and Jinan Clinical Medical Science and Technology Innovation Program (NO. 201805055, NO.201704105), and Taishan Scholar Project of Shandong Province (NO. ts201712092).

Disclosure Summary: The authors have nothing to disclose.

Abstract

Background: Graves' disease (GD) is a typical organ-specific autoimmune disease. Intestinal flora plays pivotal roles in immune homeostasis and autoimmune disease development. However, the association and mechanism between intestinal flora and GD remain elusive.

Objective: To investigate the association and mechanism between intestinal flora and GD.

Methods: We recruited 58 initially untreated GD patients and 63 healthy individuals in the study. The composition and metabolic characteristics of the intestinal flora in GD patients and the causal relationship between intestinal flora and GD pathogenesis were assessed using *16S rRNA* gene sequencing, targeted/untargeted metabolomics, and fecal microbiota transplantation (FMT).

Results: The composition, metabolism and inter-relationships of the intestinal flora were also changed, particularly the significantly reduced short-chain fatty acid (SCFA) producing bacteria and SCFAs. YCH46 strain of *Bacteroides fragilis* could produce propionic acid and increase Treg cell numbers while decrease Th17 cell numbers. Transplanting the intestinal flora of GD patients significantly increased GD incidence in GD mouse model. Additionally, three intestinal bacteria genera (*Bacteroides*, *Alistipes*, *Prevotella*) could distinguish GD patients from healthy individuals with 85% accuracy.

Conclusions: Gut dysbiosis contributes to Treg/Th17 imbalance through the pathway regulated by propionic acid and promotes the occurrence of GD together with other pathogenic factors. *Bacteroides*, *Alistipes* and *Prevotella* have great potential to serve as adjunct markers for GD diagnosis. This study provided valuable clues for improving immune dysfunction of GD patients using *B. fragilis* and illuminated the prospects of microecological therapy for GD as an adjunct treatment.

Keywords: Graves' disease, intestinal flora, Treg/Th17, *Bacteroides fragilis*, propionic acid

Abbreviations

16S rRNA, 16S ribosomal RNA; Ad-TSHR289, Adenovirus containing TSHR amino acid residues 1-289; B.f.S, The supernatant of M2GSC medium culturing B. fragilis YCH46; BMI, Body mass index; ButA, Butyryl-CoA transferase; CTAB, Cetyl trimethylammonium bromide; ELISA, Enzyme-linked immunosorbent assay; FDR, False discovery rate; FFAR2, Free fatty acid receptor 2; FMT, Fecal microbiota transplantation; FT3, free triiodothyronine; FT4, free thyroxine; GC–MS, Gas chromatography–mass spectrometry; GD, Graves' disease; GO, Graves'ophthalmopathy; HDAC, Histone deacetylase; LcdA, Lactoyl-CoA dehydratase; LEfSe, The linear discriminant analysis effect size; LPS, Lipopolysaccharides; MmdA, Methylmalonyl-CoA decarboxylase; OPLS-DA, Orthogonal partial least-squares-discriminant analysis; OUTs, Operational taxonomy units; PBMCs, Peripheral blood mononuclear cells; PBS, Phosphate buffered saline; PduP, Propionaldehyde dehydrogenase; PICRUSt, Phylogenetic Investigation of Communities by Reconstruction of Unobserved States; SCFAs, Short-chain fatty acids; TGAb, Thyroglobulin antibody; Th17, T helper 17 cell; TPOAb, Thyroperoxidase antibody; TRAb, Thyrotropin receptor antibody; Treg, Regulatory T cell; TSAb, Thyroid stimulating antibody; TSH, Thyrotropin; TSHR, TSH Receptor; TT4, Total thyroxine.

Introduction

As a typical organ-specific autoimmune disease, one of the main pathological features of Graves' disease (GD) is the presence of various antithyroid antibodies, such as thyrotropin receptor antibody (TRAb) (1). Especially, the presence of thyroid stimulating antibody (TSAb), one type of the TRAb, is the unique characteristic of GD patients. TSAb is directly responsible for the elevated level of thyroxine and GD development by stimulating the TSH receptor (2). The pathogenesis of GD is very complicated. In addition to genetic factors (1), non-genetic factors, including the environment, play key roles in the destruction of immune tolerance to thyroid tissue and autoantibody production (3). However, the exact mechanism involved in these processes has not yet been fully elucidated.

Regulatory T (Treg) cell is a subset of T helper cells and can maintain immune homeostasis by secreting inhibitory cytokines (e.g., IL-10 and TGF-β), playing pivotal roles in immune tolerance (4). The removal of Treg cells significantly increases the incidence and severity of autoimmune diseases including GD and autoimmune thyroiditis in mice (5). The number and/or function of Treg cells in the peripheral blood and thyroid of patients with GD were markedly reduced. However, some studies do not agree with the result (6). Th17 cell is also the subset of T helper cells determined by high secretion of IL-17 and other pro-inflammatory cytokines. Th17 cells are closely associated with the development of many autoimmune diseases (7-9). However, there are still conflicts about the relationship between Th17 cells and GD. Some studies showed that IL-17 and Th17 cells were increased in GD and involved in the development of GD (10). However, there are also some contradictory findings from other studies (11). The reasons for the above discrepancy may lie in the differences in animal models, races of GD patients, treatments, stages of disease, and the assay methods and/or marker molecules used for Treg and Th17 cells. Our previous study found that inhibition of retinoic acid signaling pathway caused by abnormal expression of

miRNAs was one of the important causes of Treg cell abnormalities in GD patients (12). Nevertheless, the molecular mechanism of the dysfunction of Treg and Th17 cells in GD patients is still poorly understood.

Recently, many studies have shown that gut microbiota can regulate various immune cells including Treg and Th17 in the intestinal mucosa and gastrointestinal associated lymphoid tissues (13). Additionally, various intestinal bacteria and their metabolites and constituents (such as peptide polysaccharides) can enter the circulation to regulate Treg/Th17 cells and the immune system in extra-intestinal tissues/organs. Moreover, the immune cells, including Treg and Th17 cells in the intestine, which are modulated by intestinal flora can also enter the circulation to regulate immune responses in remote tissues and organs (14). Short-chain fatty acids (SCFAs) produced by some intestinal microbes like *Bacteroides* can regulate Treg and Th17 cells in the intestine, circulation, and extra-intestinal tissues (15). Therefore, the intestinal flora is a key regulator of immune tolerance and inflammation, and plays pivotal roles in the development of various intestinal and extra-intestinal autoimmune diseases. For example, increases in the abundances of pro-inflammatory bacteria (*Escherichia coli* strains) and decreases in the abundances of anti-inflammatory bacteria (*Faecalibacterium prausnitzii*) are closely related to autoimmune intestinal diseases including Crohn's disease and ulcerative colitis (16,17). *Clostridiosis* and *Bacteroides fragilis* (*B. fragilis*) have protective effects in autoimmune encephalomyelitis mice (18,19). All these implied that gut dysbiosis might be one of the most important causes of the abnormalities in Treg and Th17 cells and impaired immune tolerance.

Diarrhea is an important clinical feature of GD and is associated with gut dysbiosis and infections of intestinal pathogenic bacteria (20,21). Many studies have shown that *Yersinia enterocolitica* is related to GD, but mice fed only with *Yersinia enterocolitica* did not develop GD (22,23). Therefore, considering the close relationship between intestinal flora and

inflammation and/or autoimmunity, very interesting questions arise as to whether gut dysbiosis is associated with abnormal immune regulation (such as the abnormalities in Treg and Th17 cells) in GD patients and what the precise mechanism underlying this association is. Recently, a study reported the compositional abnormalities in intestinal flora of GD patients and speculated the relationship between gut flora and GD development. However, the statistical methods used in this study should be optimized, and this descriptive study did not explore the mechanisms underlying the association between GD and intestinal flora (24). Therefore, more research is needed to answer the above-mentioned questions.

Herein, the profiles of gut microbiome and metabolome of GD patients were investigated using *16S rRNA* gene sequencing and targeted/non-targeted metabolomic techniques. Upon integrating with clinical data, we discovered the association between immune dysfunctions and abnormalities in the composition and metabolism of intestinal flora in GD patients, and revealed the mechanisms underlying these associations for the first time. The reduced abundance of SCFA-producing bacteria including *B. fragilis* in the intestine of GD patients markedly decreased the levels of SCFAs, especially propionic acid. These abnormalities lead to the decreased number of Tregs and increased the number of Th17 cells, resulting in the Treg/Th17 imbalance and inflammation in GD patients. This mechanism may play an important role in impaired immune tolerance and pathogenesis of GD.

Materials and Methods

Ethics statement

This study was approved by the Ethics Committee of Shandong Provincial Hospital and conformed to the principles of the Declaration of Helsinki (NO 2015-054). Informed consent was obtained from all participants. All procedures were performed in compliance with relevant laws and institutional guidelines.

Recruitment of subjects and sample collection

We recruited 58 initially untreated GD patients and 63 healthy individuals from Shandong Provincial Hospital. The two groups of subjects were matched with respect to age, sex, and body mass index (BMI). All GD patients were diagnosed according to their medical history, physical examination, and laboratory tests including thyrotropin (TSH), free triiodothyronine (FT3), free thyroxine (FT4) and TRAb based on the 2018 European Thyroid Association Guideline for the Management of Graves' Hyperthyroidism. The exclusion criteria were as follows: pregnancy, smoking, alcohol addiction, diarrhea (having loose stools three or more times in one day or watery stools) (25,26), hypertension, diabetes mellitus, lipid dysregulation, and BMI>27; usage of the following drugs within 3 months: antibiotics, probiotics, prebiotics, symbiotics, hormonal medication, laxatives, proton pump inhibitors, insulin sensitizers or Chinese herbal medicine; medical history of autoimmune diseases, malignancy and gastrointestinal tract surgery. Peripheral blood (5 mL) was collected from all subjects in the morning after an overnight fast (≥ 8 h). The serum samples were stored at -80°C for cytokine and lipopolysaccharide (LPS) detection. Peripheral blood mononuclear cells (PBMCs) were isolated using Ficoll density centrifugation (Sigma-Aldrich, St. Louis, USA). Commode Specimen Collection Kits were provided to all subjects for stool collection and the collected fecal samples were stored at −80°C after liquid nitrogen freezing.

Assays of thyroid function and thyroid-related auto-antibodies

Serum levels of TSH, FT3, FT4, thyroglobulin antibody (TGAb), thyroid peroxidase antibodies (TPOAb), and TRAb, of the recruited subjects were assayed using chemiluminescent immunoassays (ADVIA Centaur XP, Erlangen, Germany; Cobas E801 module, Roche Diagnostics, Switzerland) according to the manufacturer's instructions. Reference ranges were as follows: TSH: 0.55-4.78 μIU/mL; FT4: 11.5-22.7 pmol/L; FT3: 3.5-6.5 pmol/L; TRAb: 0.00-1.58 IU/L; TPOAb: 0.00-60 IU/mL; and TGAb: 0.00-60 IU/mL. The serum levels of TRAb and total thyroxine (TT4) in mice were measured using enzyme-linked immunosorbent assay (ELISA) kits (Jianglai biotech, Shanghai, China) and SpectraMax Microplate Reader (Molecular Devices, Sunnyvale, CA, USA) according to the manufacturer's instructions. The normal range was defined as the mean ± 3 standard deviations (SD) of mice in control group (27).

***16S rRNA* gene sequencing**

Total genome DNA was extracted from the fecal samples of 38 GD patients and 37 healthy individuals using the improved CTAB (cetyl trimethylammonium bromide) method. DNA concentration was determined using the NanoDrop 2000 (Thermo Scientific, Waltham, MA, USA) spectrophotometer. The V1-V2 regions of the *16S rRNA* gene were amplified using PCR and universal primers (Univ 27F/Univ 338R) (Table S1) (28,29). Next, the amplicons were sequenced on an Illumina HiSeq 2500 system (San Diego, California, USA) and 250 bp paired-end reads were generated.

Bioinformatic analysis of sequencing data

The raw sequencing data were merged and filtered using the fastq software. The identification and taxonomic annotation of operational taxonomic units (OTUs) were performed using the QIIME software (http://qiime.org/) and Silva 12.8 database according to the software manual (30). The linear discriminant analysis effect size (LEfSe) analysis was performed to identify differentially abundant bacterial taxa as biomarkers (LDA score>4 and $p<0.05$) (31). KEGG (Kyoto Encyclopedia of Genes and Genomes) pathways and COG (clusters of orthologous groups) functions were analyzed using the PICRUSt (Phylogenetic Investigation of Communities by Reconstruction of Unobserved States) software (32,33). Spearman correlation was calculated using R package psych. To determine if taxonomic differences in the microbiota could be used to classify samples into different cohorts and the ability of prediction, a machine learning algorithm named Random Forests was applied to analyze the genus-level abundance of gut bacteria using the R package randomForest (34).

Untargeted metabolomic analysis of stool samples

Approximately 100 mg stool was extracted with 1 mL methanol, and 60 μL 2-Chloro-L-phenylalanine and Heptadecanoic acid (0.2 mg/mL) was added as the internal standard. After vortexing, ultrasonic treatment, and centrifugation, the supernatant was transferred into a new tube and dried using vacuum concentration. Next, 60 μL methoxyamine pyridine (15 mg/mL) and N, O-bis(trimethylsilyl) trifluoro-acetamide (BSTFA) reagent were sequentially added and reacted at 37℃. After centrifugation, the supernatant was analyzed using the ACQUITY UPLC system (Waters Corporation, Milford, USA) coupled with AB SCIEX Triple TOF 5600 System (AB SCIEX, Framingham, MA, USA) in positive and negative ion modes. Data was acquired in full scan (m/z ranges from 70 to 1000) mode according to the manufacturer's instructions.

Bioinformatic analysis of metabolomic data

The raw data were converted to mzXML files using MSconvent software. All metabolite ions were normalized and the ions (RSD%<30%) were further analyzed using SIMCA 14.0 (Umetrics, Umeå, Sweden) and XCMS 1.50 software. After mean centering and unit variance scaling, orthogonal partial least-squares-discriminant analysis (OPLS-DA) was carried out to visualize the metabolic alterations among experimental groups. The peak features were selected based on the variable influence on projection (VIP) values (>1) of the normalized peak areas. These selected peak features were then used to identify the metabolites with the reference material database including HMDB, METLIN and that built by Dalian Chem Data Solution Information Technology Co., Ltd. Furthermore, the statistical significances between the two groups of metabolites were determined by t-test with FDR (false discovery rate) correction.

Targeted metabolomic analysis of SCFAs using GC–MS

All extraction procedures were performed at 4 °C to protect the volatile SCFAs. After vortexing and centrifugation, 800 μL supernatant was added to 800 μL ethyl acetate and the mixture was vortexed and centrifuged. Afterwards, isohexanoic acid was added into 600 μL upper organic phase at a final concentration of 500 μM as an internal standard. The standards of SCFAs (acetic acid, propionic acid, butyric acid, isobutyric acid, valeric acid, isovaleric acid and caproic acid) were formulated with ethyl acetate into the concentrations of 0.1, 0.5, 1, 5, 10, 20, 50, 100, 200, and 400 (μg/mL) and were added to 500 μM isohexanoic acid. Next, 1 μL SCFAs standard or sample was analyzed by a 7890A gas chromatography system coupled to a 5975C inert XL EI/CI mass spectrometry (Agilent Technologies, Santa Clara, CA, USA). Concentrations of the SCFAs were normalized according to stool weight.

PBMCs treatment and the detection of Treg and Th17 cells

The human PBMCs isolated from healthy individuals or GD patients were cultured in RPMI-1640 medium supplemented with 10% fetal bovine serum, 100 units/mL penicillin, and 100 g/mL streptomycin. Treg cells were assayed in PBMCs treated with 300 uL M2GSC medium or the supernatant of M2GSC medium culturing *B. fragilis YCH46* with the stimulation of CD3/CD28 antibody (Invitrogen, Waltham, MA, USA), TGF-β (PeproTech, NJ, USA), and IL-2 (PeproTech, NJ, USA). The procedure of Th17 assay was the same as above, except that IL-2 was changed to IL-6 (PeproTech, NJ, USA). The cells and culture supernatants were collected for flow cytometric analysis or ELISA after 3 days of culture.

Flow cytometric analysis

For Treg cell assay, PBMCs were incubated with anti-CD4-FITC (BD Bioscience, San Jose, CA, USA), anti-CD25-APC, anti-CCR9-APC (eBioscience, Waltham, MA, USA) or anti-CCR9-PE/Cyanine7 (BioLegend, San Diego, CA, USA) at 4℃ for 30 min. For Th17 cell assay, after the stimulation with Cell Stimulation Cocktail/Protein Transport Inhibitor Cocktail (eBioscience, Waltham, MA, USA) at 37℃ for 4 h, PBMCs were stained with anti-human CD4-FITC and anti-human CCR9-APC (eBioscience, Waltham, MA, USA). After fixation and permeabilization, the PBMCs were stained with anti-FOXP3-PE or IL-17-PerCP/Cy5.5 (eBioscience, Waltham, MA, USA). Finally, the stained cells were analyzed using a FACSCalibur or FACSAria Ⅱ flow cytometer (BD Biosciences, San Jose, CA, USA) and FlowJo X software.

Bacterial selective culture and species identification

Bacterial isolation was performed using the fecal samples from healthy adult males. One-gram fecal sample was homogenized in 9 mL anaerobic M2GSC medium. After a 10-fold serial dilution, 0.3 mL suspension was inoculated on the 1.5% agar plates containing M2GSC medium at 37°C for 48 h in Anaeropack Jars. Single colonies were picked and grown overnight in 10 mL M2GSC medium. Next, the gDNA of the isolated bacterium was extracted and the full length *16S rRNA* gene was amplified with PrimeSTAR Max Premix (TaKaRa, Kusatsu, Japan) using universal 16S primers (Univ 27F/Univ 1492R) (Table S1) (29). PCR products were purified and sequenced using Sanger sequencing. For species identification, the Sanger sequencing data were blasted using the BLASTN online tool (http://blast.ncbi.nlm.nih.gov/Blast.cgi).

Cytokine and LPS assays

The serum levels of cytokine IL-2, IL-18, and sCD25 were assayed using Multiplex Human Premixed Multi-Analyte Kit (R&D Systems, MN, USA) on Luminex 200 (Luminex, Austin, TX, USA) according to the manufacturer's instructions. The cytokine concentrations were calculated using a standard curve of recombinant cytokine standards. The concentrations of other cytokines including IL-10, IL-17A (eBioscience, Waltham, MA, USA; Jianglai biotech, Shanghai, China); sCD14, TGF-β (MultiSciences, Hangzhou, China); IL-6, IL-12 (Jianglai biotech, Shanghai, China), and IL-1 β (OmnimAbs, Alhambra, CA, USA) in human serum, mouse serum or culture supernatant were assayed using ELISA kits. The plates were read at 450 nm using SpectraMax Microplate Reader (Molecular Devices, Sunnyvale, CA, USA). LPS, the Gram-negative bacterial endotoxin, was quantified using the EC Endotoxin Test Kit (Bioendo, Xiamen, China) according to the manufacturer's instructions.

PCR amplification of *16S rRNA* gene of *Yersinia enterocolitica*

For detection of *Yersinia enterocolitica*, the stool samples were collected from Graves' patients with or without diarrhea and heathy individuals, and a primer set specific to its *16S rRNA* gene was used to amplify a 330 bp product (Table S1) (29). The exclusion criteria of diarrhea were as follows: diarrhea caused by food intolerance and allergy, adverse reaction to a medication, viral infection, parasitic infection, intestinal disease, gallbladder or stomach surgery (25,26). The gDNA was extracted from stool samples using the improved CTAB method. PCR reactions were performed in a DNA Thermal Cycler (Biometra TAdvanced, Jena, Germany). Cycling conditions were as follows: denaturation at 94°C for 1 min, 35 subsequent cycles consisting of heat denaturation at 98°C for 10 s, primer annealing at 55°C for 15 s, and extension at 72°C for 40 s. PCR products were visualized on 1% agarose gels stained with GelRed.

Quantitative real-time PCR

Total RNA was extracted using the TRIzol™ reagent (Invitrogen, Waltham, MA, USA) and was reverse-transcribed using the PrimeScript RT Reagent Kit (Takara, Kusatsu, Japan). Additionally, gDNA was extracted from stool samples using the improved CTAB method. Next, quantitative PCR was performed using TB Green Premix Ex Taq (Takara, Kusatsu, Japan) and specific primers (Table S1) (29) on a CFX96 Real-Time PCR System (Bio-Rad, Hercules, CA, USA). Relative gene expression was calculated by the $2^{-\Delta\Delta Ct}$ method using *16S rRNA* gene (Univ 337F/Univ 518R) or ACTB gene as an internal control.

GD mice model construction and fecal microbiota transplantation

The adenovirus containing TSHR amino acid residues 1-289 (Ad-TSHR289) and control adenovirus (Ad-Control) were purchased from Hanbio Biotechnology Co., Ltd (Shanghai, China). Female specific pathogen-free (SPF) BALB/c mice at age 6–8 weeks were purchased from the SPF Biotechnology Co., Ltd (Beijing, China) and housed in SPF conditions. All experiments were conducted in accordance with the principles and procedures outlined in the Guideline for the Care and Use of Laboratory Animals and have been approved by Ethics Committee of Shandong Provincial Hospital of Shandong University (NO. 2019-155). After 3 days of adaptive feeding, all mice except 5 mice of control group were administered a combination of four antibiotics: ampicillin, neomycin-sulfate, metronidazole, and vancomycin (Sigma-Aldrich, St. Louis, USA) via oral gavage for 5 days (10 mg of each antibiotic per mouse per day), followed by *ad libitum* administration in drinking water (ampicillin, neomycin, and metronidazole: 1 g/L; vancomycin: 500 mg/L) (35). The antibiotic treatment lasted 2 weeks (35). The weight of the mice was measured during the antibiotic treatment. The depletion of gut flora was confirmed using *16S rRNA* gene sequencing. The mice were then transplanted with the intestinal flora of GD patients or healthy individuals. The colonization of gut microbiota in recipient mice was verified using *16S rRNA* gene sequencing after FMT. In detail, the fresh fecal samples collected from healthy individuals or GD patients were mixed with sterile normal saline and homogenized. The homogenates were then passed through a 20 μm pore filter to remove the particulate and fibrous matter. The filtrates (400 mg/mL) were used for transplantation (36). Mice were administered 200 μL of the filtrates via oral gavage once a day for a week, followed by once every two days for the remaining 6 weeks. After the first week of FMT, the mice transplanted with different intestinal flora were respectively injected in the quadriceps with 50 uL phosphate-buffered saline (PBS) containing 10^9 particles of Ad-TSHR289 or control adenovirus twice at 3-week

intervals (37,38). During the experiment, the mice of control group were orally gavaged or injected with PBS by following the same procedure for the mice of experimental groups. Blood was harvested 3 weeks after the second immunization from the tail vein for corresponding analysis.

Statistical Analysis

Data are presented as the mean±SD or median (IQR). The Mann–Whitney U test or unpaired t-test with appropriate correction for multiple comparisons was used to detect significances for continuous outcomes. For categorical variables, the chi square test or Fisher exact test were performed. $P<0.05$ was considered as statistically significant. FDR (false discovery rate) corrected p-value (q-value) <0.05 was deemed to be significant for some specific analysis. All experiments were repeated independently at least three times.

Results

Significant abnormalities in peripheral cytokines, Treg and Th17 cells of GD patients in association with the intestine

In this study, 58 initial patients with GD (GD group) and 63 healthy individuals (control group) were recruited. The demographic characteristics of all the subjects are presented in Table 1. Compared with healthy individuals, the percentage of Treg (CD4+CD25+FOXP3+) cells in CD4+ T cells was significantly lower while the percentage of Th17 (CD4+IL17+) cells in CD4+ T cells was markedly higher, resulting in a significantly decreased ratio of Treg/Th17 in the peripheral blood of GD patients (Fig. 1A-1C). CCR9 is one of the most important intestinal homing markers. CCR9 positive cells indicate that they are derived from the intestine or closely related to the intestine (39,40). We found that the proportion of

CCR9+ Treg cells in CD4+ T cells or in Treg cells was significantly decreased (Fig. 1D, 1E), while the proportion of CCR9+ Th17 cells in CD4+ T cells or in Th17 cells was significantly increased in peripheral blood of GD patients (Fig. 1F, 1G). Furthermore, compared to healthy individuals, the levels of serum anti-inflammatory cytokines (TGF-β and IL-10) were markedly decreased, while the levels of serum pro-inflammatory cytokines including sCD14, sCD25, IL-2, IL-17A, IL-1β, IL-6, and IL-12 were significantly increased in GD patients (Fig. 1H-1P). Additionally, the serum IL-18 level, which plays pivotal roles in intestinal inflammation, was also significantly elevated in GD patients (Fig. 1Q). All these results suggested that the immune and inflammatory state of the GD patients were significantly changed and these changes may be associated with the intestine.

Gut microbiota of GD patients markedly differed from that of healthy individuals

To clarify the roles of gut microbiota in the pathogenesis of GD, fecal samples were analyzed using *16S rRNA* gene sequencing. The sequencing depth was saturated (Goods coverage>0.99) and was not significantly different in GD and control groups (Fig. 2A). The parameters of richness (Ace and Chao1) and diversity (Shannon and Simpson indices) of the intestinal flora were all significantly lower in GD patients than in healthy controls, indicating a markedly decreased α diversity (Fig. 2B). Moreover, the Pielou and Simpson indexes were significantly negatively correlated with the serum levels of TRAb, FT3, and FT4 and positively correlated with the serum TSH level, indicating the significant association between the intensity of the disease and the intestinal flora (Fig. 2C). The Bray-Curtis distance-based community analysis, which is an indicator to characterize the similarity of microbial composition between individuals, showed a noticeable separation between the samples of healthy individuals and GD patients, revealing that the microbiota composition differed significantly between the two groups (Fig. 2D). At the phylum level, *Firmicutes* were less abundant while *Bacteroidetes* were more abundant (Fig. 2E), which were further confirmed

with quantitative PCR (qPCR) (Fig. 2F), thereby the ratio of *Firmicutes/Bacteroidetes* decreased significantly in GD patients (Fig. 2G). Meanwhile, the abundances of many other bacterial phyla including *Proteobacteria*, *Saccharibacteria* and *Verrucomicrobia* in GD patients were also markedly changed compared with those in the healthy individuals (Fig. 2E). At the genus level of the intestinal bacteria (abundance>0.2%), the abundance of 33 bacterial genera were significantly decreased while 7 bacterial genera were markedly increased in GD patients, and they all belonged to *Firmicutes*, *Proteobacteria* and *Bacteroidetes* (Fig. 2H). LEfSe analysis demonstrated that the genus *Bacteroides* (*g_Bacteroides*) enriched in healthy individuals was one of the top four biomarkers. However, the phylum *Bacteroidetes* (*p_Bacteroidetes*), order *Bacteroidales* (*o_Bacteroidales*) and class *Bacteroidia* (*c_Bacteroidia*) were enriched in GD patients (Fig. 2I, 2J). The random forest analysis also showed that three intestinal bacteria (*Bacteroides*, *Alistipes*, *Prevotella*) could distinguish GD patients from healthy individuals with 85% accuracy (Fig. 3A, 3B). These findings indicated that *Bacteroides* might play an important role in the occurrence of GD. Additionally, *Yersinia enterocolitica* is an enteropathogenic bacterium and is frequently reported in GD patients. However, it was not detected in our *16S rRNA* gene sequencing data. To explain this result, qPCR was performed on fecal samples from different individuals and showed that the detection rate of *Yersinia enterocolitica* was significantly higher in GD patients with diarrhea than in GD patients without diarrhea and healthy individuals (Fig. 4A, 4B).

Gut dysbiosis can seriously interfere with the interactions among intestinal bacteria. The correlations between abundances of bacteria are good reflections of the interactions among bacteria. Our results demonstrated that the correlations among many intestinal bacteria of GD patients were significantly changed. In healthy individuals, the probiotic *Lactobacillus* which is considered to play an important role in physical health and be involved in autoimmune

diseases (41,42), was positively correlated with SCFA-producing bacteria (such as *Desulfovibrio, Veillonella*), but these correlations were weakened or even disappeared in GD patients. Additionally, the probiotic *Bacteroides*, which could produce SCFAs was negatively correlated with the pathogenic bacteria *Prevotella*_2 in healthy individuals, while this relationship disappeared in GD patients. Another genus producing propionic acid, *Dialister*, was negatively correlated with *Streptococcus* in healthy individuals, but this correlation became positive in GD patients (Fig. 5A). These changes of correlations among the microflora might be closely related to the development of GD, but more research is still needed to reveal their significance and mechanism.

To clarify the pathological significance of these significantly altered intestinal bacteria in GD patients, the correlations between their relative abundances and the clinical features of GD (serum levels of FT3, FT4, TPOAb, TGAb, TRAb, and TSH) were analyzed. The results showed that *Proteobacteria, Tenericutes, Lentisphaerae, Verrucomicrobia*, and *Synergistetes* were negatively correlated with the serum levels of FT3, FT4, TPOAb, and TRAb, while positively correlated with the serum TSH level. *Hydrogenedentes, Bacteroidetes, Saccharibacteria,* and *Spirochaetae* demonstrated the exact opposite of the above results (Fig. 5B). At the genus level, intestinal bacteria except *Streptococcus*, *Alloprevotella*, *Veillonella*, *Neisseria*, *Acinetobacter*, *Prevotella* and *Prevotella*_7 were significantly negatively correlated with the serum levels of TPOAb, TRAb, FT3, and FT4, but positively correlated with the serum TSH level (Fig. 5C). Among the altered bacteria with significant association with the clinical indicators of GD, the abundance of *Bacteroides* was considerably higher than that of other genera (Fig. 5D). Additionally, the serum level of LPS was significantly increased in GD patients (Fig. 5E), implying that intestinal dysbiosis in GD patients might result in the intestinal barrier disruption.

Gut metabolites including SCFAs were significantly changed in GD patients

Gut metabolites are important bridges for intestinal flora to regulate the host immune system. Therefore, metabolomic analysis was performed to explore the intestinal metabolic profiles of GD patients. A total of 540 and 578 peak features were identified, respectively in positive ion mode (ES+) and negative ion mode (ES-). These peak features were clustered by orthogonal partial least squares discriminant analysis (OPLS-DA), showing that the samples of control and GD groups were clearly separated from each other (Fig. 6A, 6B). A total of 292 (112 upregulated peaks and 180 downregulated peaks) and 225 (134 upregulated peaks and 91 downregulated peaks) peak features were significantly changed in the ES+ and ES- modes, respectively (Fig. 6C). These findings indicated that the intestinal metabolic profiles in GD patients changed markedly. The significantly changed peak features were analyzed using MS/MS and many metabolites were identified by the combination of precise molecular weight and structural information of compound structure database. These metabolites included amino acid derivatives, lipids, fatty acids, bile acids, and many of them were significantly changed in GD patients (Fig. 6D, 6E).

The results of PICRUSt showed that the predicted relative abundances of butanoate and propanoate metabolism were significantly lower in GD patients (Fig. 6F). Therefore, the volatile SCFAs in the intestine were detected by GC-MS and the results showed that propionic acid and butyric acid, two important immunomodulatory SCFAs, were significantly decreased in GD patients compared with those in healthy individuals. Moreover, the reduction of propionic acid was the *most significant in these SCFAs* (Fig. 6G). The intestinal levels of other SCFAs including acetic, isobutyric, valeric acid and isovaleric acids in GD were decreased without statistical significance (Fig. 6G, 6H).

Close correlations among clinical features of GD, SCFAs, and SCFA-producing bacteria

To explore the significance of the perturbations in intestinal flora and metabolites, 52 differential metabolites with the most statistical significance were selected and the Spearman correlation coefficients between them (a part of them) and the clinical features of GD (the significantly changed bacteria) were calculated. Many altered metabolites were significantly correlated with the changed intestinal flora ($|r|>0.5$, corrected $p<0.05$). Propionate and Butyrate were significantly positively correlated with many SCFA-producing bacteria including *Roseburia*, *Bacteroides*, *Phascolarctobacterium*, *Alistipes*, *Lachnospiraceae NK4A136*, *Christensenellaceae R-7*, *Ruminococcaceae_UCG-005*, *Ruminococcaceae_UCG-002*, *Turicibacter*, and *Ruminococcus* (Fig. 7A). In addition, many remarkably changed intestinal metabolites were significantly correlated with the clinical indicators of GD. Propionate which significantly decreased in the gut of GD patients was strongly negatively correlated with the serum levels of TPOAb, FT3, FT4, and TRAb, while strongly positively correlated with the serum level of TSH, which suggested that propionate was closely related to the condition of patients with GD. Moreover, dihydroxyacetone representing high metabolic rate, was significantly positively correlated with the serum levels of FT3 and TRAb (Fig. 7B).

ButA (butyryl-CoA transferase), LcdA (lactoyl-CoA dehydratase), PduP (propionaldehyde dehydrogenase), and MmdA (methylmalonyl-CoA decarboxylase) are the key enzymes to produce butyric acid and propionic acid in gut flora. In intestinal flora of GD patients, the abundances of these key enzyme-encoding genes were all significantly decreased, confirming the significant reduction in their SCFA-producing ability and resulting in the lack of SCFAs in GD patients (Fig. 7C). The qPCR using the primers specific for the representative bacteria of SCFA-producing genera showed that the abundance of *Bacteroides fragilis* species was the

most closely related to the levels of TRAb, FT3, FT4, and TSH and decreased with the most statistical significance in the intestine of GD patients (Fig. 7D, 7E).

Bacteroides fragilis modulates Treg/Th17 balance through the pathway regulated by propionic acid

To elucidate the role and mechanism of *B. fragilis* in immune dysfunction, such as Treg/Th17 imbalance in GD patients, the strains of *B. fragilis* were isolated from human feces using a selective culture medium M2GSC in anaerobic conditions and confirmed as *B. fragilis YCH46* strain with 100% identity using Sanger sequencing. qPCR also showed that the abundance of *B. fragilis YCH46* strain in GD patients was significantly reduced compared to that in healthy controls (Fig. 8A). Compared to M2GSC medium, the supernatant of M2GSC medium culturing *B. fragilis YCH46* (B.f.S) could significantly increase the percentage of CD4+CD25+FOXP3+ Treg cells and IL-10 level, while reduce the percentage of CD4+IL17+ Th17 cells and IL-17A level in PBMCs from healthy individuals (Fig. 8B-8D). Moreover, B.f.S could improve the imbalance of Treg/Th17 in patients with GD (Fig. 8E-8G). Propionic acid is well known as the important metabolite produced by *B. fragilis*. Our results showed that the expression of *FFAR2* (a propionic acid receptor) mRNA was markedly upregulated, while the expression of histone deacetylase 6 and histone deacetylase 9 mRNA, which are the downstream molecules of *FFAR2* and could suppress Treg cells, were downregulated in PBMCs from both healthy individuals and GD patients treated with B.f.S (Fig. 8H, 8I). These results indicated that *B. fragilis YCH46* could influence the differentiation and/or proliferation of Treg and Th17 cells through the pathway regulated by propionic acid, and then modulate the Treg/Th17 balance.

Intestinal flora contributed to the development of GD revealed by fecal microbiota transplantation in mouse model

To clarify the causal relationship between gut dysbiosis and GD pathogenesis, fecal microbiota transplantation (FMT) was performed using a mouse model of GD. The experimental procedure was shown in Fig. 9A. The results showed that the broad-spectrum antibiotic treatment effectively removed most of the gut bacteria in mice, while did not significantly affect mice body weight (Fig. S2A, S2B) (29). The PCoA results showed that the sample points representing the intestinal flora from the donor individuals and the corresponding recipient mice were almost completely overlapped, indicating the bacteria colonization was successful after FMT (Fig. S2C, S2D) (29). The mouse model was constructed by transfecting the adenovirus containing TSHR amino acid residues 1-289 (Ad-TSHR289) (37,43). The results showed that transfection of the blank adenovirus vector (Ad-control) had no significant effect on the thyroid function (serum total T4 level) and immuno-inflammation (serum levels of TRAb, IL-17A, and IL-10) in the mice. On the contrary, transfecting Ad-TSHR289 significantly increased the serum levels of TT4, TRAb and IL-17A, and decreased serum IL-10 level in the mice (Fig. 9B-9E). These results indicated that the GD mouse model was successfully established. Moreover, FMT showed that the transplantation of fecal microbiota from healthy individuals or GD patients had similar effects on the thyroid function and immuno-inflammation of the mice transfected with Ad-control (Fig. 9F-9I). However, in the mice transfected with Ad-TSHR289, the transplantation of intestinal flora of GD patients significantly elevated the serum levels of TT4, TRAb, and IL-17A and decreased the serum IL-10 level compared to transplanting the intestinal flora of healthy individuals (Fig. 9J-9M), and increased the GD incidence from 28.6% to 73.3% (Fig. 9N). These results indicate that abnormal intestinal flora alone may not be sufficient to cause thyroid dysfunction and GD development. However, it can significantly promote the

occurrence and development of GD together with other pathogenic factors. Thus, intestinal flora abnormality is one of the important pathogenic factors of GD, not just its consequence or accompanying phenomenon.

Discussion

In this study, we revealed for the first time that intestinal flora abnormality is one of the important pathogenic factors in the development and immune abnormalities of GD. The composition, metabolism and inter-relationships of intestinal flora in GD patients were considerably reshaped with significant relations to the clinical features of GD, including the decreased abundance of SCFA-producing bacteria and SCFAs. Intestinal *B. fragilis* could modulate the balance between Treg and Th17 cells through its metabolite propionic acid. The reduction in *B. fragilis* contributed to the imbalance of Th17 and Treg cells, thereby promoting the pathogenesis of GD.

Until now many studies have demonstrated the complex interactions between the gut flora and the host (44). Recently, the concept of gut-thyroid axis has been proposed (45). However, the regulatory mechanism between the gut and thyroid is still not fully elucidated, and the gut bacteria involved in the development of GD have rarely been reported. A recent descriptive study reported changes in the composition of intestinal flora in GD patients, but did not explore the mechanism and causal relationship between these changes and GD (24). Another study also reported the association between the serum TRAb level and the intestinal microbiota in patients with Graves' orbitopathy (GO) (46). Our FMT results for the first time proved that although abnormal intestinal flora alone may not be sufficient to cause thyroid dysfunction and GD development, it could markedly promote the occurrence and development of GD together with other pathogenic factors. Thus, intestinal flora abnormality

is one of the important mechanisms for GD pathogenesis. With regard to the mechanism through which the gut regulates thyroid function, most previous studies were focused on the molecular mimicry of bacteria (22). Our results imply that in addition to molecular mimicry, the immune regulation of intestinal flora is a novel mechanism through which the gut regulates thyroid function, namely how the gut-thyroid axis works. Additionally, although *Yersinia enterocolitica* is considered to be involved in the development of GD through different mechanisms including molecular mimicry, we did not detect it using *16S rRNA* gene sequencing. The main reason may be that in this study, we excluded the GD patients with diarrhea similar to other studies on gut microbiota using *16S rRNA* gene sequencing, because diarrhea can markedly change the composition of the intestinal flora. In fact, we found that *Yersinia enterocolitica* was easy to detect in only GD patients with diarrhea. Another reason may be the differences in the assay methods; serological assay was used often in the previous studies in which *Yersinia enterocolitica* was detected in GD patients, while *16S rRNA* gene sequencing was used in this study. *Yersinia enterocolitica* was also not detected in the recently published studies, which analyzed the intestinal flora of GD and GO patients using *16S rRNA* gene sequencing (24,46).

The decrease in Treg cells and increase in Th17 cells in peripheral blood of GD patients have been reported previously (47). However, the mechanism of these abnormalities has not been fully elucidated. CCR9 is one of the most important gut homing markers and CCR9+ cells are likely to be derived from, or closely related to the intestine (39,40). In this study, we found that a high proportion of the peripheral Treg and Th17 cells were CCR9 positive. Moreover, the changes in CCR9+Treg and CCR9+Th17 cells were almost the same as the changes in total Treg and Th17 cells in peripheral blood of GD patients. This implied that the abnormalities of peripheral Treg and Th17 cells in GD patients were mainly caused by the cells derived from the intestine, and were closely related to the intestine and intestinal flora.

This also suggested that in GD patients, the gut flora might regulate the Treg and Th17 cells mainly in the intestine, and then the regulated cells enter the circulation and play immunomodulatory roles outside the gut.

B. fragilis is one of the most frequent species at the human intestinal mucosal surface, and plays pivotal roles in the development of the host immune system (48). We found that its abundance was significantly decreased in the gut of GD patients. Moreover, the supernatant of the medium culturing the YCH46 strain of *B. fragilis* (B.f.S) containing high concentration of propionic acid could increase the ratio of Treg/Th17 in PBMCs of both healthy individuals and GD patients. This indicated that *B. fragilis* could produce propionic acid, which might be the important mechanism of its immunomodulatory effects (49). Some studies have reported that propionic acid could regulate immune cell activation, proliferation, and differentiation through G-protein coupled receptors (such as GPR41, GPR43) and histone deacetylase (HDAC) (15). We found that the expression of *GPR43* (*FFAR2*) mRNA was significantly upregulated, while the expression of *HDAC6* and *HDAC9* mRNAs was significantly downregulated in PBMCs of both healthy individuals and GD patients treated with B.f.S. This suggested that propionic acid produced by *B. fragilis* might inhibit *HDACs* through *GPR43* (*FFAR2*) and regulate Treg and Th17 cells. In addition to directly regulating the inflammatory and immune responses, SCFAs, including propionic acid, can also affect gut barrier integrity (50). Our study showed that the plasma level of bacterial LPS was markedly increased in GD patients, implying the gut barrier dysfunction, which is closely related to the immune abnormalities of GD patients (51). Its mechanism may be that the reduction in SCFA-producing bacteria leads to a decrease in SCFAs, which impairs gut barrier integrity.

Due to the lack of effective early warning indicators, most GD patients are diagnosed and treated after noticeable clinical symptoms appeared (52). At this moment, the best time window for intervention has been missed and it is difficult to eliminate the immune

abnormalities that cause GD. Our study identified a few intestinal bacteria that significantly changed in the gut of GD patients. The result of random forest showed that a group of intestinal bacteria (*Bacteroides*, *Alistipes*, *Prevotella*) could accurately differentiate GD patients from healthy individuals with 85% accuracy. Since gut dysbacteriosis is one of the important causes of GD, the abnormalities of intestinal flora are likely to occur before the clinical symptoms and/or classic indicators of GD appear. Therefore, these three intestinal bacteria have potential as markers for diagnosis of GD.

Recurrence is a major problem for GD therapy and 40-60% of GD patients are reported to relapse after treatment (53). Its main cause might be that the factors causing immune dysfunction have not been effectively removed and the immune function has not been restored. Intestinal flora is a key regulator of immune function and can be used as a therapeutic target for improving immune function in GD patients. In recent years, the efficacy of microecological therapy, which targets the intestinal flora and includes fecal microbiota transplantation, probiotic, or prebiotic treatments, is increasingly being recognized in the treatment of chronic metabolic diseases and autoimmune diseases (54). According to our findings, YCH46 strain of *B. fragilis* was a natural inhibitor of Th17 cells and activator of Treg cells, and could ameliorate the immune dysfunction in GD patients *in vitro*, indicating it could be used as an immunomodulator and an auxiliary treatment for GD patients to reduce the recurrence rate. The therapeutic potential of *B. fragilis YCH46* warrants a comprehensive study to assess its efficacy and safety.

Conclusions

In summary, our study revealed the role and mechanism of gut microbiota in the immune dysfunction of GD (Fig. 10) and identified three intestinal bacteria, which have potential as adjunct markers for GD diagnosis. This study also provided valuable insights for improving immune dysfunction in GD patients using *B. fragilis* and illuminated the prospect of microecological therapy for GD. The combination therapy of microecology and drug could be a powerful candidate for reducing recurrence of GD.

Acknowledgments

This work was supported by the National Natural Science Foundation of China (NO. 81570712 and 81670247) and the Natural Science Outstanding Youth Foundation of Shandong Province (NO. JQ201519), Major Science and Technology Innovation Project of Shandong Province (NO. 2018CXGC1218) and Jinan Clinical Medical Science and Technology Innovation Program (NO. 201805055, NO.201704105), and Taishan Scholar Project of Shandong Province (NO. ts201712092). We would like to thank Xinjie Zhang for her help in the experiments.

Data Availability

The datasets generated during and/or analyzed during the current study are not publicly available but are available from the corresponding author on reasonable request.

Disclosure Statement

The authors declare no competing financial interests.

References

1. Davies TF, Andersen S, Latif R, Nagayama Y, Barbesino G, Brito M, Eckstein AK, Stagnaro-Green A, Kahaly GJ. Graves' disease. *Nature reviews Disease primers*. 2020;6(1):52.
2. Barbesino G, Tomer Y. Clinical review: Clinical utility of TSH receptor antibodies. *J Clin Endocrinol Metab*. 2013;98(6):2247-2255.
3. Prummel MF, Strieder T, Wiersinga WM. The environment and autoimmune thyroid diseases. *Eur J Endocrinol*. 2004;150(5):605-618.
4. Göschl L, Scheinecker C, Bonelli M. Treg cells in autoimmunity: from identification to Treg-based therapies. *Seminars in immunopathology*. 2019;41(3):301-314.
5. Saitoh O, Nagayama Y. Regulation of Graves' hyperthyroidism with naturally occurring CD4+CD25+ regulatory T cells in a mouse model. *Endocrinology*. 2006;147(5):2417-2422.
6. Nakano A, Watanabe M, Iida T, Kuroda S, Matsuzuka F, Miyauchi A, Iwatani Y. Apoptosis-induced decrease of intrathyroidal CD4(+)CD25(+) regulatory T cells in autoimmune thyroid diseases. *Thyroid*. 2007;17(1):25-31.
7. Yasuda K, Kitagawa Y, Kawakami R, Isaka Y, Watanabe H, Kondoh G, Kohwi-Shigematsu T, Sakaguchi S, Hirota K. Satb1 regulates the effector program of encephalitogenic tissue Th17 cells in chronic inflammation. *Nature communications*. 2019;10(1):549.
8. Cho JJ, Xu Z, Parthasarathy U, Drashansky TT, Helm EY, Zuniga AN, Lorentsen KJ, Mansouri S, Cho JY, Edelmann MJ, Duong DM, Gehring T, Seeholzer T, Krappmann D, Uddin MN, Califano D, Wang RL, Jin L, Li H, Lv D, Zhou D, Zhou L, Avram D. Hectd3 promotes pathogenic Th17 lineage through Stat3 activation and Malt1 signaling in neuroinflammation. *Nature communications*. 2019;10(1):701.
9. Takeuchi Y, Hirota K, Sakaguchi S. Impaired T cell receptor signaling and development of T cell-mediated autoimmune arthritis. *Immunol Rev*. 2020;294(1):164-176.
10. Li Q, Wang B, Mu K, Zhang JA. The pathogenesis of thyroid autoimmune diseases: New T lymphocytes - Cytokines circuits beyond the Th1-Th2 paradigm. *Journal of cellular physiology*. 2019;234(3):2204-2216.
11. Yuan Q, Zhao Y, Zhu X, Liu X. Low regulatory T cell and high IL-17 mRNA expression in a mouse Graves' disease model. *J Endocrinol Invest*. 2017;40(4):397-407.
12. Wang Z, Fan X, Zhang R, Lin Z, Lu T, Bai X, Li W, Zhao J, Zhang Q. Integrative analysis of mRNA and miRNA array data reveals the suppression of retinoic acid pathway in regulatory T cells of Graves' disease. *J Clin Endocrinol Metab*. 2014;99(12):E2620-2627.
13. Britton GJ, Contijoch EJ, Mogno I, Vennaro OH, Llewellyn SR, Ng R, Li Z, Mortha A, Merad M, Das A, Gevers D, McGovern DPB, Singh N, Braun J, Jacobs JP, Clemente JC, Grinspan A, Sands BE, Colombel JF, Dubinsky MC, Faith JJ. Microbiotas from Humans with Inflammatory Bowel Disease Alter the Balance of Gut Th17 and RORγt(+) Regulatory T Cells and Exacerbate Colitis in Mice. *Immunity*. 2019;50(1):212-224.e214.
14. Omenetti S, Pizarro TT. The Treg/Th17 Axis: A Dynamic Balance Regulated by the Gut

Microbiome. *Front Immunol*. 2015;6:639.

15. Smith PM, Howitt MR, Panikov N, Michaud M, Gallini CA, Bohlooly YM, Glickman JN, Garrett WS. The microbial metabolites, short-chain fatty acids, regulate colonic Treg cell homeostasis. *Science*. 2013;341(6145):569-573.
16. Hornef MW, Pabst O. Real friends: Faecalibacterium prausnitzii supports mucosal immune homeostasis. *Gut*. 2016;65(3):365-367.
17. Viladomiu M, Kivolowitz C, Abdulhamid A, Dogan B, Victorio D, Castellanos JG, Woo V, Teng F, Tran NL, Sczesnak A, Chai C, Kim M, Diehl GE, Ajami NJ, Petrosino JF, Zhou XK, Schwartzman S, Mandl LA, Abramowitz M, Jacob V, Bosworth B, Steinlauf A, Scherl EJ, Wu HJ, Simpson KW, Longman RS. IgA-coated E. coli enriched in Crohn's disease spondyloarthritis promote TH17-dependent inflammation. *Sci Transl Med*. 2017;9(376).
18. Lee YK, Menezes JS, Umesaki Y, Mazmanian SK. Proinflammatory T-cell responses to gut microbiota promote experimental autoimmune encephalomyelitis. *Proceedings of the National Academy of Sciences of the United States of America*. 2011;108 Suppl 1:4615-4622.
19. Ochoa-Reparaz J, Mielcarz DW, Wang Y, Begum-Haque S, Dasgupta S, Kasper DL, Kasper LH. A polysaccharide from the human commensal Bacteroides fragilis protects against CNS demyelinating disease. *Mucosal immunology*. 2010;3(5):487-495.
20. Miller LJ, Owyang C, Malagelada JR, Gorman CA, Go VL. Gastric, pancreatic, and biliary responses to meals in hyperthyroidism. *Gut*. 1980;21(8):695-700.
21. Hodges K, Gill R. Infectious diarrhea: Cellular and molecular mechanisms. *Gut Microbes*. 2010;1(1):4-21.
22. Wang Z, Zhang Q, Lu J, Jiang F, Zhang H, Gao L, Zhao J. Identification of outer membrane porin f protein of Yersinia enterocolitica recognized by antithyrotopin receptor antibodies in Graves' disease and determination of its epitope using mass spectrometry and bioinformatics tools. *J Clin Endocrinol Metab*. 2010;95(8):4012-4020.
23. Weiss M, Ingbar SH, Winblad S, Kasper DL. Demonstration of a saturable binding site for thyrotropin in Yersinia enterocolitica. *Science*. 1983;219(4590):1331-1333.
24. Ishaq HM, Mohammad IS, Shahzad M, Ma C, Raza MA, Wu X, Guo H, Shi P, Xu J. Molecular Alteration Analysis of Human Gut Microbial Composition in Graves' disease Patients. *Int J Biol Sci*. 2018;14(11):1558-1570.
25. DuPont HL. Acute infectious diarrhea in immunocompetent adults. *N Engl J Med*. 2014;370(16):1532-1540.
26. Thapar N, Sanderson IR. Diarrhoea in children: an interface between developing and developed countries. *Lancet (London, England)*. 2004;363(9409):641-653.
27. Ueki I, Abiru N, Kawagoe K, Nagayama Y. Interleukin 10 deficiency attenuates induction of anti-TSH receptor antibodies and hyperthyroidism in a mouse Graves' model. *J Endocrinol*. 2011;209(3):353-357.
28. Carvalho FA, Koren O, Goodrich JK, Johansson ME, Nalbantoglu I, Aitken JD, Su Y, Chassaing B, Walters WA, Gonzalez A, Clemente JC, Cullender TC, Barnich N, Darfeuille-Michaud A, Vijay-Kumar M, Knight R, Ley RE, Gewirtz AT. Transient inability to manage

proteobacteria promotes chronic gut inflammation in TLR5-deficient mice. *Cell Host Microbe*. 2012;12(2):139-152.

29. Su XH, Yin XL, Liu Y, Yan XF, Zhang SC, Wang XW, Lin ZW, Zhou XM, Gao J, Wang Z, Zhang QY. Data from: Gut dysbiosis contributes to the imbalance of Treg and Th17 cells in Graves' disease patients by propionic acid. figshare. Deposited 17 July 2020. Dataset. https://doi.org/10.6084/m9.figshare.12661646.v1
30. Caporaso JG, Kuczynski J, Stombaugh J, Bittinger K, Bushman FD, Costello EK, Fierer N, Pena AG, Goodrich JK, Gordon JI, Huttley GA, Kelley ST, Knights D, Koenig JE, Ley RE, Lozupone CA, McDonald D, Muegge BD, Pirrung M, Reeder J, Sevinsky JR, Turnbaugh PJ, Walters WA, Widmann J, Yatsunenko T, Zaneveld J, Knight R. QIIME allows analysis of high-throughput community sequencing data. *Nat Methods*. 2010;7(5):335-336.
31. Segata N, Izard J, Waldron L, Gevers D, Miropolsky L, Garrett WS, Huttenhower C. Metagenomic biomarker discovery and explanation. *Genome Biol*. 2011;12(6):R60.
32. Langille MG, Zaneveld J, Caporaso JG, McDonald D, Knights D, Reyes JA, Clemente JC, Burkepile DE, Vega Thurber RL, Knight R, Beiko RG, Huttenhower C. Predictive functional profiling of microbial communities using 16S rRNA marker gene sequences. *Nature biotechnology*. 2013;31(9):814-821.
33. Parks DH, Tyson GW, Hugenholtz P, Beiko RG. STAMP: statistical analysis of taxonomic and functional profiles. *Bioinformatics*. 2014;30(21):3123-3124.
34. Giannini HM, Ginestra JC, Chivers C, Draugelis M, Hanish A, Schweickert WD, Fuchs BD, Meadows L, Lynch M, Donnelly PJ, Pavan K, Fishman NO, Hanson CW, 3rd, Umscheid CA. A Machine Learning Algorithm to Predict Severe Sepsis and Septic Shock: Development, Implementation, and Impact on Clinical Practice. *Critical care medicine*. 2019;47(11):1485-1492.
35. Kuss SK, Best GT, Etheredge CA, Pruijssers AJ, Frierson JM, Hooper LV, Dermody TS, Pfeiffer JK. Intestinal microbiota promote enteric virus replication and systemic pathogenesis. *Science*. 2011;334(6053):249-252.
36. Wei YL, Chen YQ, Gong H, Li N, Wu KQ, Hu W, Wang B, Liu KJ, Wen LZ, Xiao X, Chen DF. Fecal Microbiota Transplantation Ameliorates Experimentally Induced Colitis in Mice by Upregulating AhR. *Front Microbiol*. 2018;9:1921.
37. Chen CR, Aliesky HA, Guo J, Rapoport B, McLachlan SM. Blockade of costimulation between T cells and antigen-presenting cells: an approach to suppress murine Graves' disease induced using thyrotropin receptor-expressing adenovirus. *Thyroid*. 2006;16(5):427-434.
38. Nagayama Y, Saitoh O, McLachlan SM, Rapoport B, Kano H, Kumazawa Y. TSH receptor-adenovirus-induced Graves' hyperthyroidism is attenuated in both interferon-gamma and interleukin-4 knockout mice; implications for the Th1/Th2 paradigm. *Clinical and experimental immunology*. 2004;138(3):417-422.
39. Kadowaki A, Saga R, Lin Y, Sato W, Yamamura T. Gut microbiota-dependent CCR9+CD4+ T cells are altered in secondary progressive multiple sclerosis. *Brain : a journal of neurology*. 2019;142(4):916-931.

40. Hoeppli RE, MacDonald KN, Leclair P, Fung VCW, Mojibian M, Gillies J, Rahavi SMR, Campbell AIM, Gandhi SK, Pesenacker AM, Reid G, Lim CJ, Levings MK. Tailoring the homing capacity of human Tregs for directed migration to sites of Th1-inflammation or intestinal regions. *American journal of transplantation : official journal of the American Society of Transplantation and the American Society of Transplant Surgeons*. 2019;19(1):62-76.
41. Servin AL. Antagonistic activities of lactobacilli and bifidobacteria against microbial pathogens. *FEMS Microbiol Rev*. 2004;28(4):405-440.
42. Fine RL, Mubiru DL, Kriegel MA. Friend or foe? Lactobacillus in the context of autoimmune disease. *Advances in immunology*. 2020;146:29-56.
43. Liu L, Wu L, Gao A, Zhang Q, Lv H, Xu L, Xie C, Wu Q, Hou P, Shi B. The Influence of Dihydrotestosterone on the Development of Graves' Disease in Female BALB/c Mice. *Thyroid*. 2016;26(3):449-457.
44. Elzinga J, van der Oost J, de Vos WM, Smidt H. The Use of Defined Microbial Communities To Model Host-Microbe Interactions in the Human Gut. *Microbiology and molecular biology reviews : MMBR*. 2019;83(2).
45. Lerner A, Jeremias P, Matthias T. Gut-thyroid axis and celiac disease. *Endocr Connect*. 2017;6(4):R52-R58.
46. Shi TT, Xin Z, Hua L, Zhao RX, Yang YL, Wang H, Zhang S, Liu W, Xie RR. Alterations in the intestinal microbiota of patients with severe and active Graves' orbitopathy: a cross-sectional study. *J Endocrinol Invest*. 2019;42(8):967-978.
47. Li C, Yuan J, Zhu YF, Yang XJ, Wang Q, Xu J, He ST, Zhang JA. Imbalance of Th17/Treg in Different Subtypes of Autoimmune Thyroid Diseases. *Cell Physiol Biochem*. 2016;40(1-2):245-252.
48. Wexler HM. Bacteroides: the good, the bad, and the nitty-gritty. *Clin Microbiol Rev*. 2007;20(4):593-621.
49. Rios-Covian D, Sanchez B, Salazar N, Martinez N, Redruello B, Gueimonde M, de Los Reyes-Gavilan CG. Different metabolic features of Bacteroides fragilis growing in the presence of glucose and exopolysaccharides of bifidobacteria. *Front Microbiol*. 2015;6:825.
50. Felizardo RJF, Watanabe IKM, Dardi P, Rossoni LV, Câmara NOS. The interplay among gut microbiota, hypertension and kidney diseases: The role of short-chain fatty acids. *Pharmacological research*. 2019;141:366-377.
51. Girgis CM, Champion BL, Wall JR. Current concepts in graves' disease. *Ther Adv Endocrinol Metab*. 2011;2(3):135-144.
52. Ginsberg J. Diagnosis and management of Graves' disease. *CMAJ : Canadian Medical Association journal = journal de l'Association medicale canadienne*. 2003;168(5):575-585.
53. Mao XM, Li HQ, Li Q, Li DM, Xie XJ, Yin GP, Zhang P, Xu XH, Wu JD, Chen SW, Wang SK. Prevention of relapse of Graves' disease by treatment with an intrathyroid injection of dexamethasone. *J Clin Endocrinol Metab*. 2009;94(12):4984-4991.
54. Borody TJ, Khoruts A. Fecal microbiota transplantation and emerging applications. *Nat Rev Gastroenterol Hepatol*. 2011;9(2):88-96.

Table 1: Demographic and clinical characteristics of GD patients and healthy individuals

	Control	GD	P value
Number	63	58	
Sex (M/F)	28/35	23/35	ns
Age (Y)	43.86 ± 9.20	42.07 ± 10.22	ns
BMI (kg/m^2)	22.49 ± 2.25	22.48 ± 2.48	ns
FT3 (pml/L)	4.85 (0.58)	16.94 (21.71)	****
FT4 (pmol/L)	15.83 (2.18)	48.89 (54.23)	****
TSH (μIU/mL)	1.92 (1.29)	0.005 (0.005)	****
TRAb (IU/L)	0.54 (0.47)	11.98 (22.94)	****
TGAb (IU/mL)	23.20 (9.50)	67.70 (379.37)	***
TPOAb (IU/mL)	33.10 (8.60)	206.75 (1253.15)	****

Data are shown as the mean±SD and median (Interquartile Range, IQR). The Chi-Squared test (Sex), t-test (Age and BMI) and Mann–Whitney U test (FT3, FT4, TSH, TRAb, TGAb and TPOAb) were used to detect significant changes. ns: not significant; ***: $p<0.001$, ****: $p<0.0001$.

Control: healthy individuals; GD: Graves' disease patients; M: male; F: female; Y: year; BMI: Body Mass Index; FT3: free T3; FT4: free T4; TSH: thyrotropin; TRAb: thyrotropin receptor antibody; TGAb: thyroglobulin antibody; TPOAb: thyroperoxidase antibody.

Figure 1: Abnormalities of cytokines, Treg, and Th17 cells in the peripheral blood of GD patients. (A, B) The percentages of Treg (CD4+CD25+FOXP3+) cells (A) and Th17 (CD4+IL17+) cells (B) in CD4+ T cells of healthy individuals (control) and GD patients (GD). **(C)** The ratio of Treg/Th17 cells in the peripheral blood of control and GD groups. **(D, E)** The percentages of CCR9+ Treg cells (CCR9+CD4+CD25+FOXP3+) in CD4+ T cells (D) or in Treg cells (CD4+CD25+FOXP3+) (E) in the peripheral blood of control and GD groups. **(F, G)** The percentages of CCR9+ Th17 cells (CCR9+CD4+IL17+) in CD4+ T cells (F) or in Th17 cells (CD4+IL17+) (G) in the peripheral blood of control and GD groups. **(H-Q)** The serum levels of anti-inflammatory cytokines TGF-β (H), IL-10 (I) and pro-inflammatory cytokines sCD14 (J), sCD25 (K), IL-2 (L), IL-17A (M), IL-1β (N), IL-6 (O), IL-12 (P), and IL-18 (Q) in control and GD groups were assayed using Luminex and ELISA. Data are presented as the mean ± SD or median (IQR). The t-test (I, K, and N) and Mann–Whitney U test (A-H, J, and L-Q) were used to detect significant differences. *: P<0.05; **: P<0.01; ***: P<0.001; ****: P<0.0001.

Figure 2: Significant changes in the gut microbiota composition of GD patients. (A) Average number of sequencing reads in healthy individuals (control) and GD patients (GD). **(B)** The α diversity indices (Ace, Chao1, Shannon and Simpson indexes) of the intestinal flora in healthy individuals (control) and GD patients (GD). **(C)** Heatmap of the correlations between major clinical indicators of GD and the Pielou and Simpson indexes of intestinal flora. The color bar with numbers indicates the correlation coefficients. The FDR-adjusted P-values by t-test were shown by asterisks (***: corrected p<0.001). TSH: thyrotropin; TRAb: thyrotropin receptor antibody; FT3: free triiodothyronine; FT4: free thyroxine. **(D)** Non-metric multidimensional scaling (NMDS) plot based on Bray-Curtis distance matrix of

control and GD groups. Each point represents a sample. The ellipses do not represent statistical significance, but rather serve as a visual guide to group diff erences. **(E)** The relative abundances of intestinal bacteria at the phylum level in control and GD groups. **(F)** The fold changes in the abundances of *Firmicutes* and *Bacteroidetes* in intestinal flora of GD group compared with that of control group. They were determined using qPCR. **(G)** The ratio of *Firmicutes/Bacteroidetes* in GD patients and healthy individuals was calculated using the *16S rRNA* gene sequences data. **(H)** Heatmap of the relative abundances of intestinal bacteria with significant differences (corrected $p<0.05$ by Mann–Whitney U test) at the genus level in control and GD groups. The color bar indicates Z score, which represents the relative abundance. Z score<0 (>0) means the relative abundance was lower (higher) than the mean. The color bar on the left represents the phyla of intestinal bacteria. Pink: *Bacteroidetes*; Green: *Firmicutes*; Brick red: *Proteobacteria*. **(I)** Cladogram generated by LEfSe analysis. The significantly differential bacterial clades or taxa are highlighted. Red: increased abundance in GD group. Green: increased abundance in control group. **(J)** LDA scores of the intestinal bacteria in control and GD groups at different taxonomic levels generated using LEfSe analysis. LDA score>4 or <-4 means bacterial taxa are significantly enriched in control group (green) or GD group (red) ($p<0.05$). p: phylum; c: class; o: order; f: family; g: genus; s: species. Data are presented as the median (IQR). The t-test (A) and Mann–Whitney U test (B, E, F, G, I and J) were used to detect significant changes. ns: not significant; *: P<0.05; **: P<0.01; ***: P<0.001; ****: P<0.0001.

Figure 3: Random forest analysis. (A) Results of the Random Forests analysis. The bacterial genera that could significantly discriminate between GD patients (GD) and healthy individuals (control) were presented in descending order. Three bacterial genera that could

accurately distinguish GD patients and healthy individuals with 85% accuracy were indicated by rectangle. **(B)** Graphic representation of the classifier accuracy per sample group/cohort.

Figure 4: Detection rate of *Yersinia enterocolitica* in healthy individuals and GD patients with and without diarrhea. (A) The agarose electrophoresis of PCR products of *Yersinia enterocolitica* amplified in fecal samples from healthy individuals (lanes 1, 2, 3, 4, and 5), GD patients without diarrhea (lanes 6, 7, 8, 9, 10, and 11) and GD patients with diarrhea (lanes 12, 13, 14, 15, 16, 17, 18, and 19). Lane M: DNA marker. **(B)** Comparisons of the detection rate of *Yersinia enterocolitica* in the intestinal flora of healthy individuals and GD patients with and without diarrhea. Statistical analysis was performed using Fisher's exact test. The detection rate of *Yersinia enterocolitica* was significantly higher in GD patients with diarrhea than in healthy individuals and GD patients without diarrhea.

Figure 5: Correlation network of gut microbiota and correlation analysis of clinical indicators and intestinal bacteria, as well as serum LPS level. (A) Correlation network of gut microbiota in healthy individuals (control) and GD patients (GD). The significant strong correlations ($|r|>0.3$ and corrected $p<0.05$ by t-test) among the intestinal bacterial genera are presented in the network. The red and green edges represent the positive correlations and negative correlations, respectively. The spot colors represent different bacterial phyla. The thickness of the edges represents the strength of the correlation. The dotted rectangles indicate that the bacteria are emphasized in the Results section. **(B)** Heatmap of correlations between six clinical indicators of GD and the abundances of intestinal bacterial phyla. The bacterial phyla emphasized in text are marked with rectangles. **(C)** Heatmap of the correlations between six clinical indicators of GD and the top 40 most abundant bacterial

genera whose abundance significantly changed in GD patients. In B and C, the color bar with numbers indicates the correlation coefficients, and the FDR-adjusted P-values using t-test are shown by asterisks (*: corrected p<0.05; **: corrected p<0.01; ***: corrected p<0.001). TSH: thyrotropin; TGAb: thyroglobulin antibody; TPOAb: thyroperoxidase antibody; TRAb: thyrotropin receptor antibody; FT3: free triiodothyronine; FT4: free thyroxine. **(D)** Comparisons of the relative abundances of the top ten most abundant bacterial genera which were significantly correlated with the clinical indicators of GD. **(E)** Serum levels of LPS in GD patients (GD) and healthy individuals (control) measured using the LAL test. Data are presented as the median (IQR). The Mann–Whitney U test was used to detect significant changes for D and E. *: P<0.05; **: P<0.01; ***: P<0.001; ****: P<0.0001.

Figure 6: Noticeable changes in the metabolic profiles of gut microbiota in GD patients. **(A)** The plot of OPLS-DA score of all peak features from the untargeted metabolomics analysis of stool samples of healthy individuals (control) and GD patients (GD). **(B)** Validation of the OPLS-DA model via permutation test (times = 200). The criterion for model validity was that the regression line of the Q2-points (blue dotted line) intersected the vertical solid line (on the left) below zero. **(C)** Cloud plots of the peak features of intestinal metabolites which significantly changed in GD patients in positive ion mode (ES+, upper panel) and negative ion mode (ES-, under panel). Red (blue) circles indicate the significantly increased (decreased) metabolites (fold change>1.5, p<0.05) in the stool samples of GD patients. The color tone indicates p-values: the darker the color tone, the larger the p-value. The radius of circle indicates the fold changes of corresponding peak features. **(D)** Heatmap of the relative abundance of the top 50 most abundant metabolites which significantly changed in GD group (corrected p<0.05 by t-test). The color bar indicates Z score, which represents the relative abundance. Z score<0 (>0) meant the relative abundance was lower

(higher) than the mean. **(E)** Comparisons of the relative amounts of some representative intestinal metabolites in GD and control groups. **(F)** The significant differences in metagenomics functions in GD patients (GD) compared to that in healthy individuals (control) (corrected $p<0.05$ and confidence intervals=95%). This analysis was performed using PICRUSt software. **(G)** The concentrations of propionic acid, butyric acid and acetic acid in fecal samples of control and GD groups were determined by GC-MS. **(H)** The concentrations of isobutyric acid, isovaleric acid, and valeric acid in the fecal samples from healthy individuals (control) and GD patients (GD). Data are presented as the mean ± SD or median (IQR). The t-test (C, E and F) and Mann–Whitney U test (G and H) were used to detect significant differences. ns: not significant; *: $P<0.05$; **: $P<0.01$; ***: $P<0.001$; ****: $P<0.0001$.

Figure 7: Correlations among intestinal bacteria, metabolites, and clinical indicators of GD, as well as the changes in SCFA-producing genera and key enzymes for producing butyric acid and propionic acid. (A) Heatmap of correlations between the significantly changed bacterial genera and eight metabolites with important functions and significant differences. The color bar with numbers indicates the correlation coefficients. The important bacterial genera are marked with rectangles. **(B)** Heatmap of correlations between six clinical indicators of GD and the remarkably changed intestinal metabolites in GD patients. The color bar with numbers indicates the correlation coefficients. The important metabolites are marked with rectangles. **(C)** The abundance changes in the key enzymes for producing butyric acid and propionic acid in the intestinal flora of GD patients (GD) and healthy individuals (control). ButA, Butyryl-CoA transferase; LcdA, lactoyl-CoA dehydratase; PduP, propionaldehyde dehydrogenase; MmdA, methylmalonyl-CoA decarboxylase. **(D)** Heatmap of correlations between six clinical indicators of GD and the abundance of the nine

representative SCFA-producing bacteria, which significantly changed in GD patients. The color bar with numbers indicates the correlation coefficients. **(E)** The abundance changes in the nine representative SCFA-producing bacteria in intestinal flora of GD patients (GD) and healthy individuals (control). They were determined using qPCR. Data are presented as the median (IQR). The FDR-adjusted P-values by t-test are shown by asterisks for A, B and D. *: corrected p<0.05; **: corrected p<0.01; ***: corrected p<0.001 in A, B and D. The Mann–Whitney U test was used to detect significant differences for C and E. ns: not significant; **: P< 0.01; ***: P<0.001.

Figure 8: Treg/Th17 balance is modulated by *Bacteroides fragilis* through the pathway regulated by propionic acid. (A) Changes in the abundance of *Bacteroides fragilis YCH46* strain in the intestinal flora of the control and GD groups was determined using qPCR. **(B, C)** PBMCs from healthy individuals were treated with M2GSC medium (M2GSC) or the supernatant of M2GSC medium culturing *B. fragilis YCH46* (B.f.S) for 72 h. Then, the percentage of Treg (CD4+CD25+FOXP3+) and Th17 cells (CD4+IL17+) in CD4+ T cells were analyzed using flow cytometry. **(D)** The concentrations of IL-10 and IL-17A in the culture medium of healthy individuals' PBMCs treated with M2GSC or B.f.S. **(E, F)** PBMCs from GD patients were treated as described above. The percentage of Treg (CD4+CD25+FOXP3+) and Th17 cells (CD4+IL17+) in CD4+ T cells were analyzed by flow cytometry. **(G)** The concentrations of IL-10 and IL-17A in the culture medium of GD patients' PBMCs treated with M2GSC or B.f.S. **(H, I)** The fold changes in mRNA expression of *FFAR2*, *HDAC6*, and *HDAC9* in PBMCs from healthy individuals (H) or GD patients (I) treated with B.f.S compared to that treated with M2GSC. The experiment was repeated at least three times independently. Data are presented as the median (IQR). The Mann–Whitney

U test was used to detect significant differences. *: P<0.05; **: P<0.01; ***: P<0.001; ****: P<0.0001.

Figure 9: Fecal microbiota transplantation (FMT) in the mouse model of GD. (A) The schematic diagram of the experimental process including FMT and immunization. FMT-C: transplanting fecal microbiota from healthy individuals; FMT-GD: transplanting fecal microbiota from GD patients. Ad-Control: control adenovirus; Ad-TSHR289: adenovirus containing TSHR amino acid residues 1-289. **(B-M)** The serum levels of total T4 (TT4, B, F, J), TRAb (C, G, K), IL-17A (D, H, L) and IL-10 (E, I, M) were measured at 3 weeks after the second immunization. **(N)** Comparison of the incidences of thyroid dysfunction in different groups. The levels of serum TT4 and TRAb more than the values, namely their corresponding mean + 3SD of the mice immunized with Ad-Control (control group) were considered as abnormal and GD development. GD+: mice with GD; GD-: mice without GD. In B-M, the mice in control group were treated as described in the Materials and Methods. The mice transfected with Ad-Control were Ad-Control group (Ad-Control). The mice transfected with Ad-TSHR289 were Ad-TSHR289 group (Ad-TSHR289). Transplanting the fecal microbiota from healthy individuals (GD patients) to the mice transfected with Ad-Control was FMT-C+Ad-Control (FMT-GD+Ad-Control) group. Transplanting the fecal microbiota from healthy individuals (GD patients) to the mice transfected with Ad-TSHR289 was FMT-C+Ad-TSHR289 (FMT-GD+Ad-TSHR289) group. Data are presented as the median (IQR). Kruskal-Wallis test with Steel Dwass in B-M and Fisher's exact test in N were used to detect significant changes. ns: not significant; *: corrected P<0.05; **: corrected P<0.01; ***: corrected P<0.001; ****: corrected P<0.0001.

Figure 10: Schematic representation of the mechanism through which gut microbiota modulates Treg/Th17 balance and contributes to the development of GD. The blue downward arrows indicate downregulation/decrease. The red upward arrows indicate upregulation/increase.

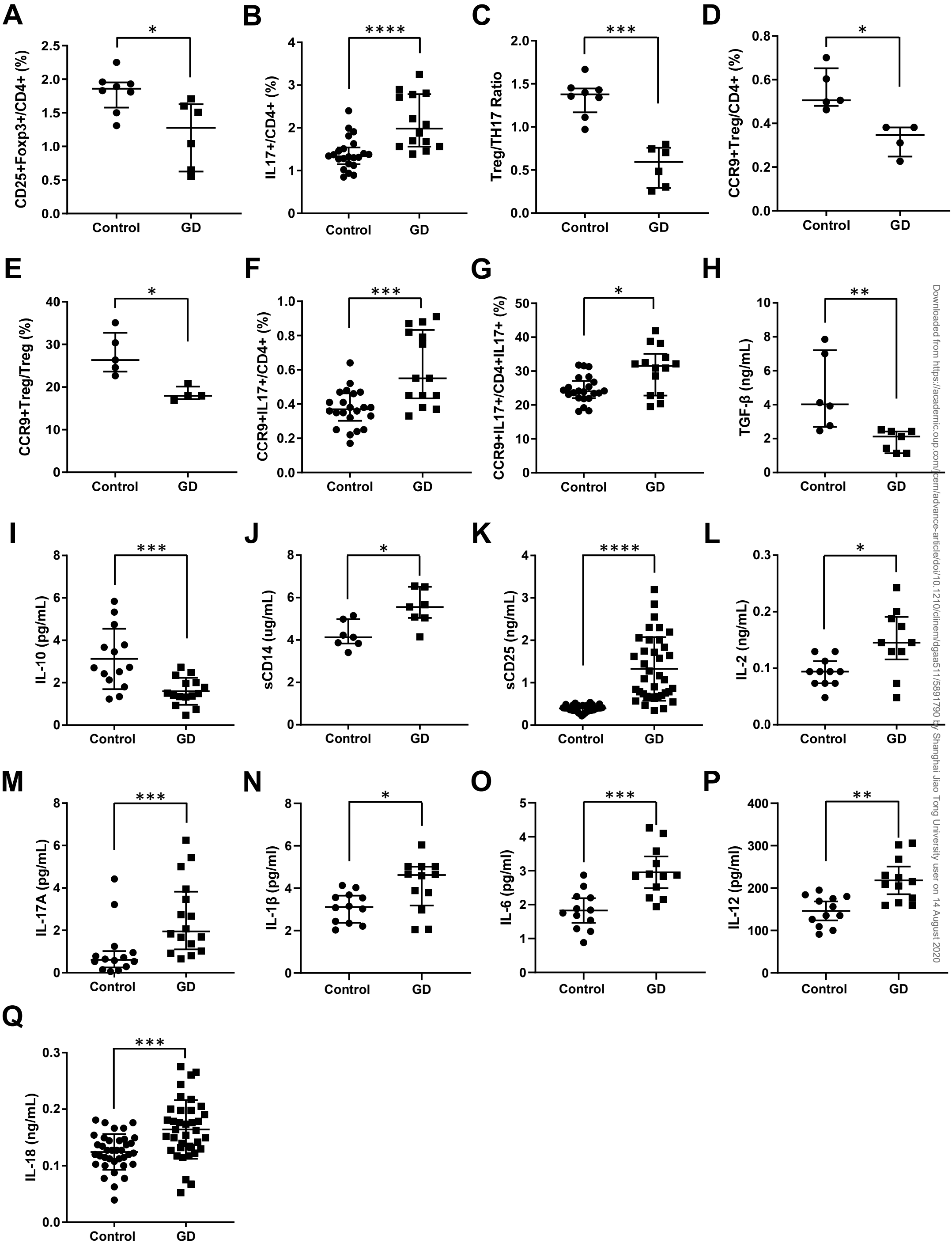

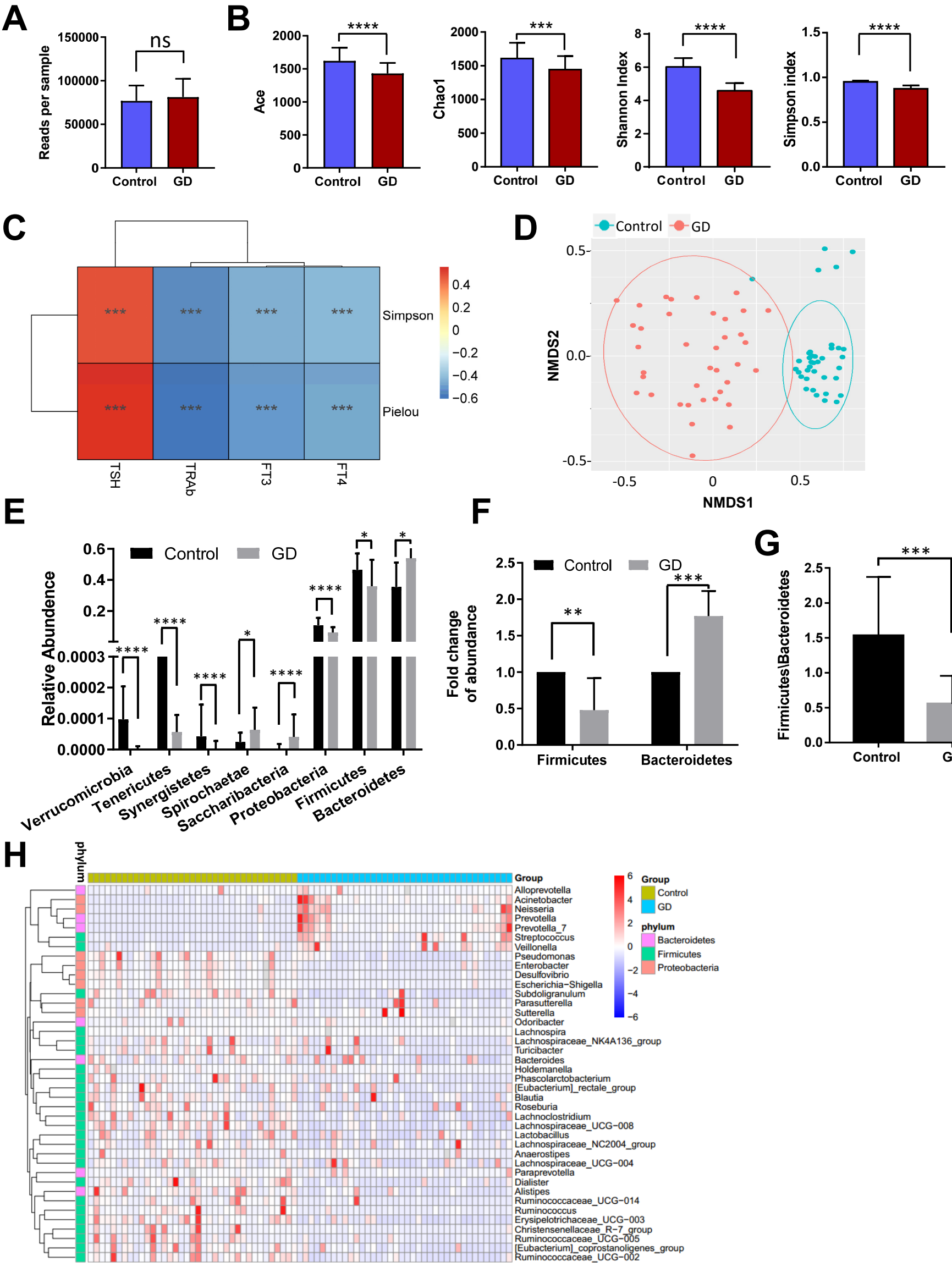

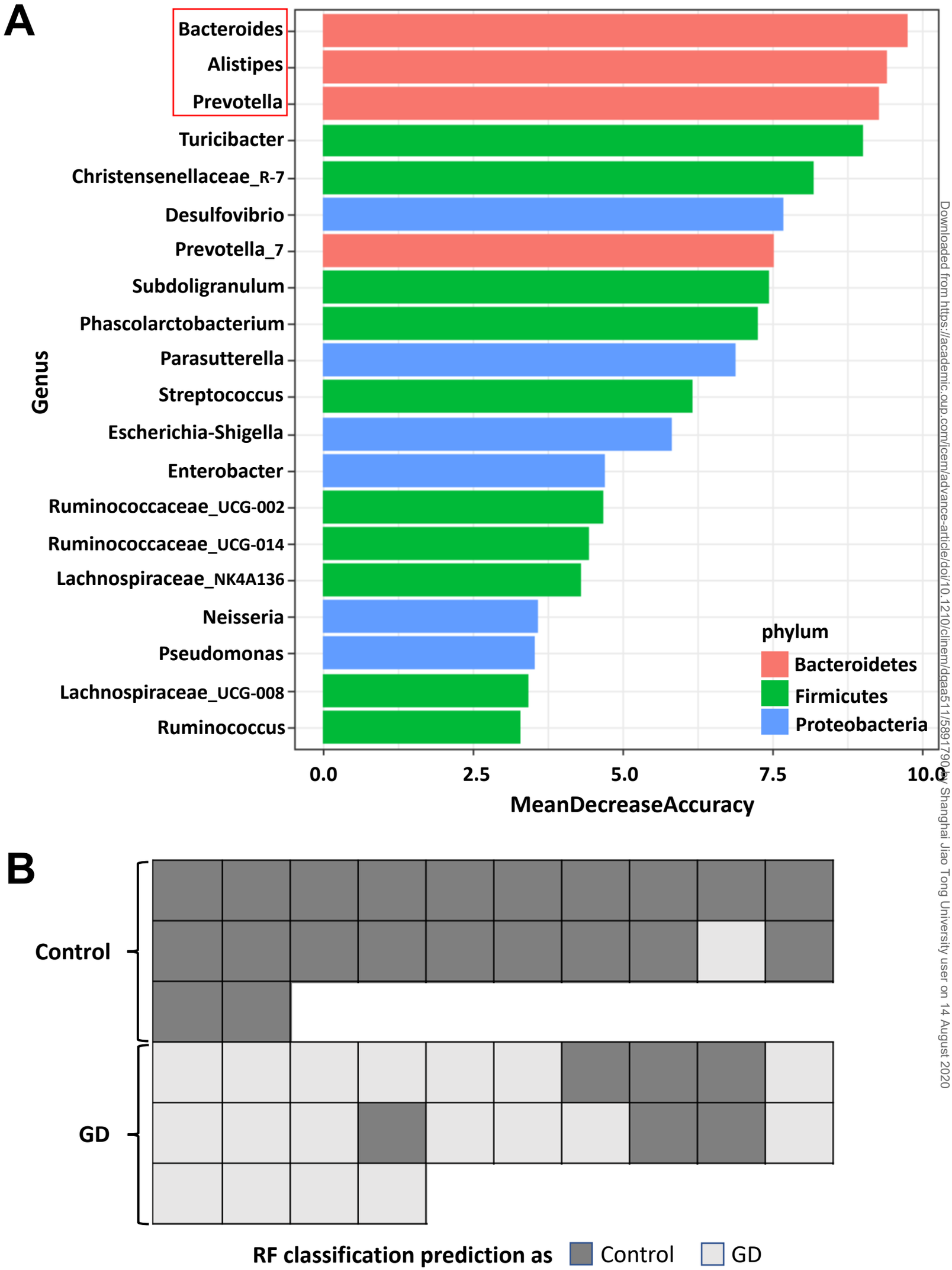

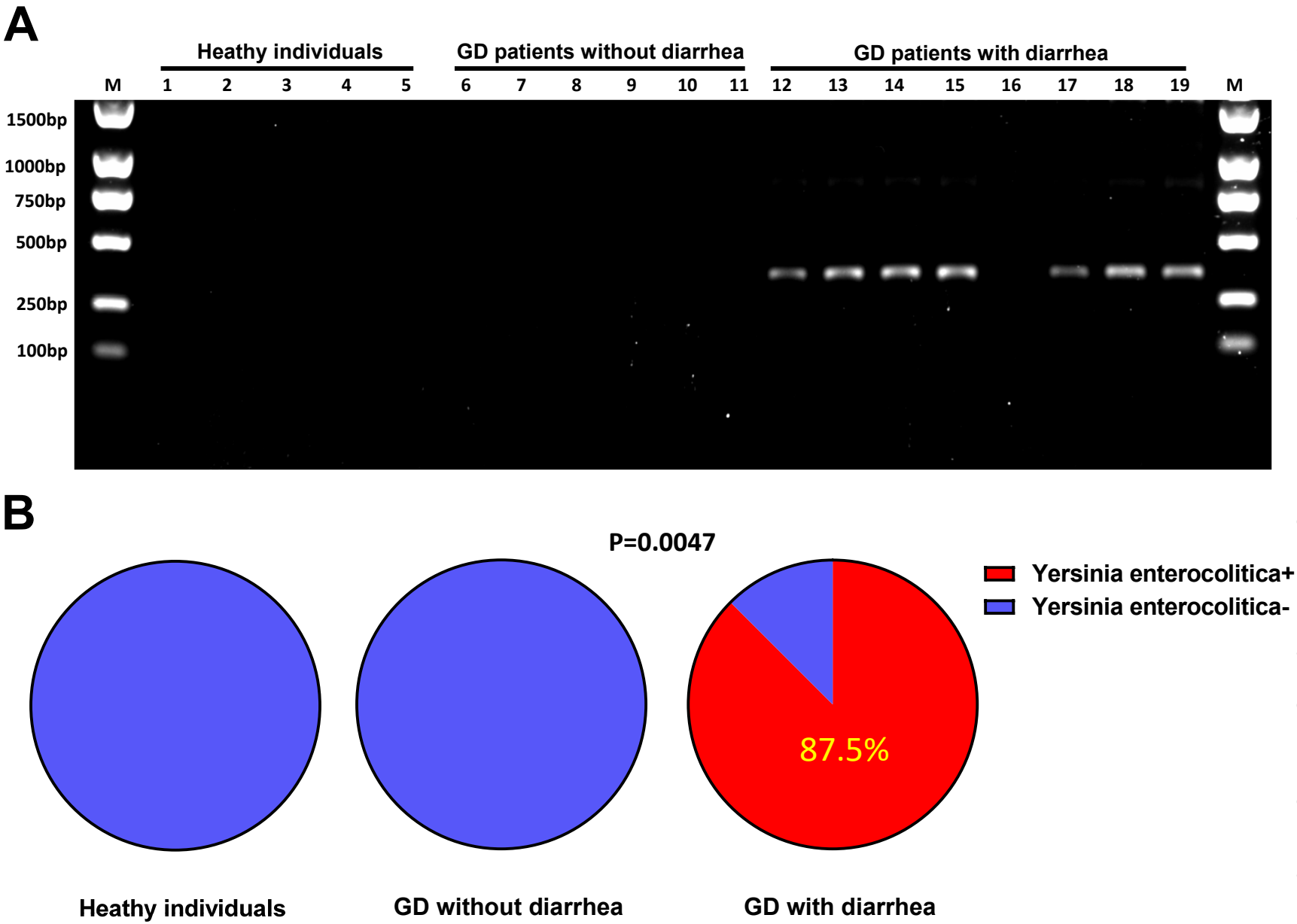

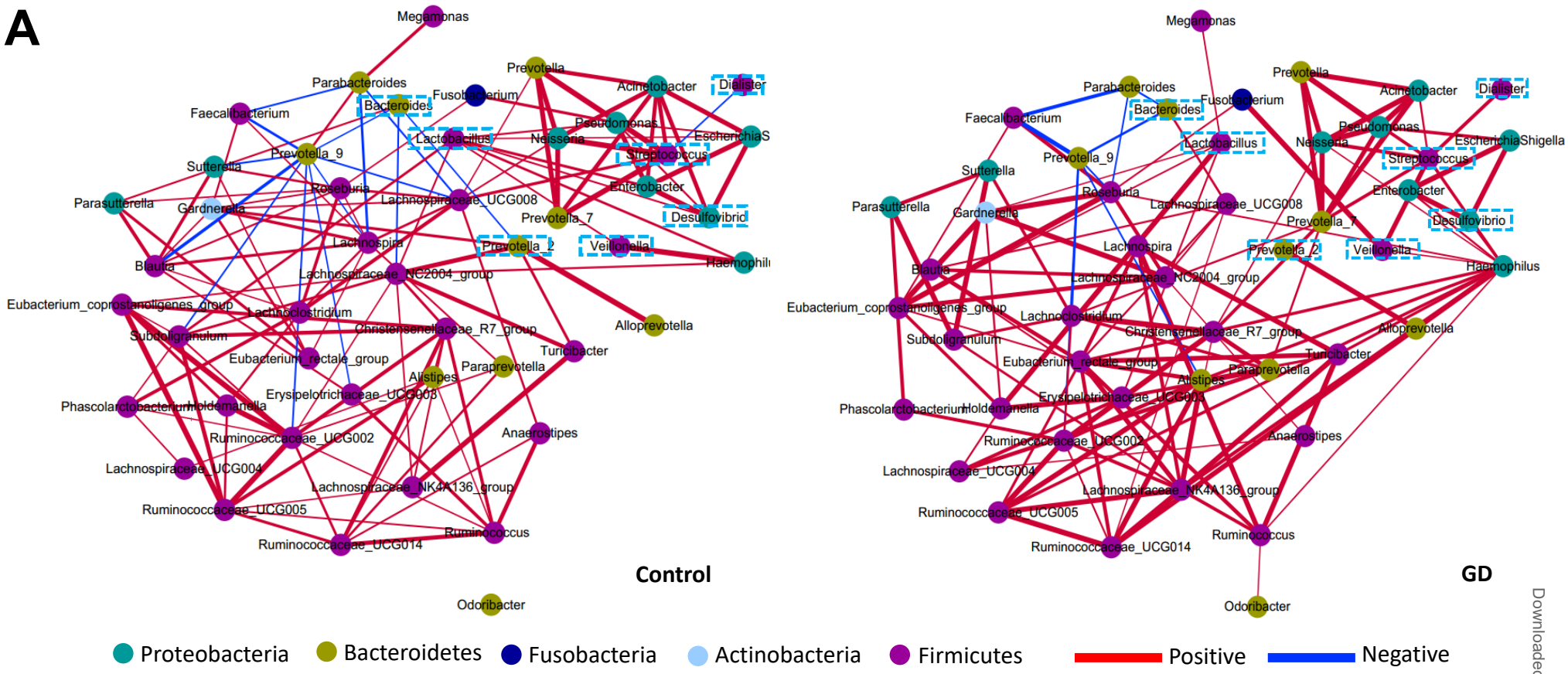

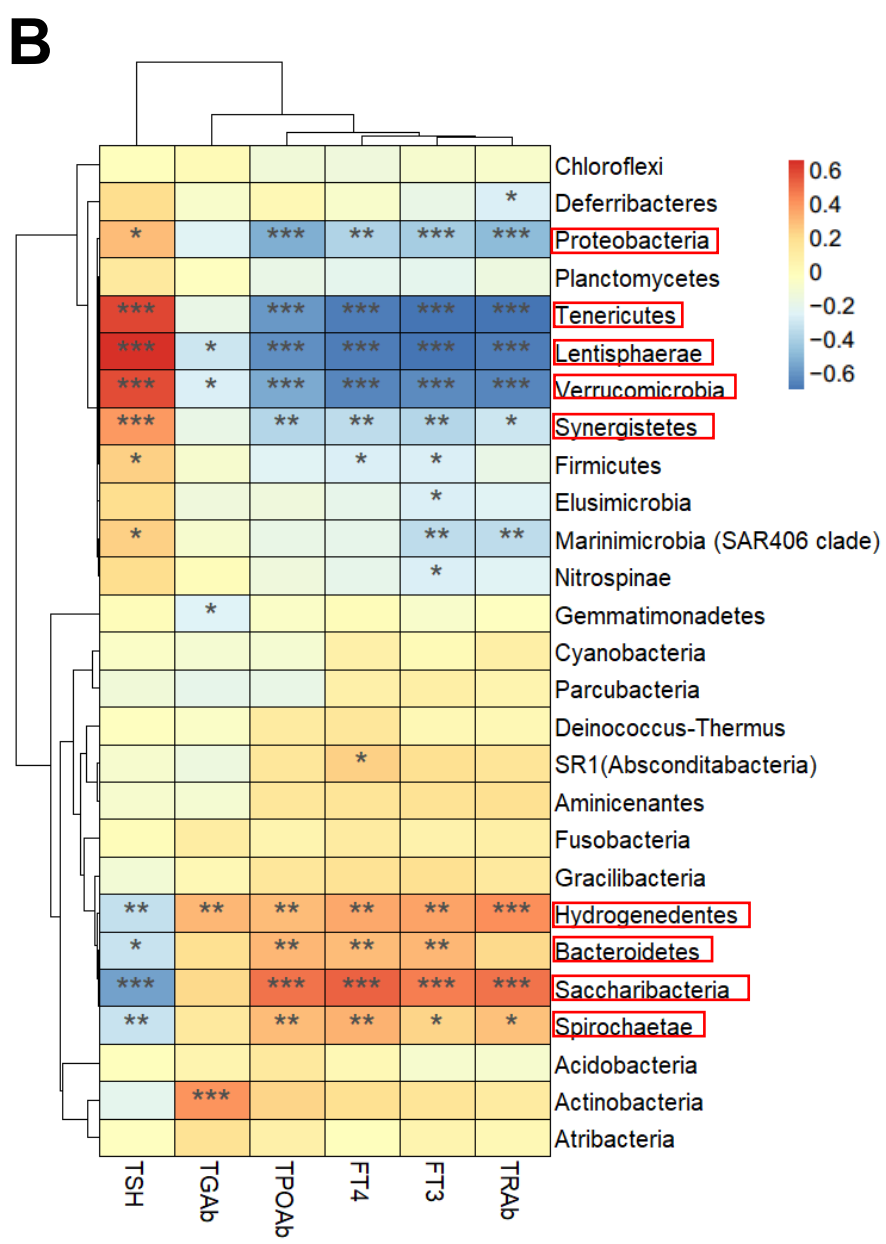

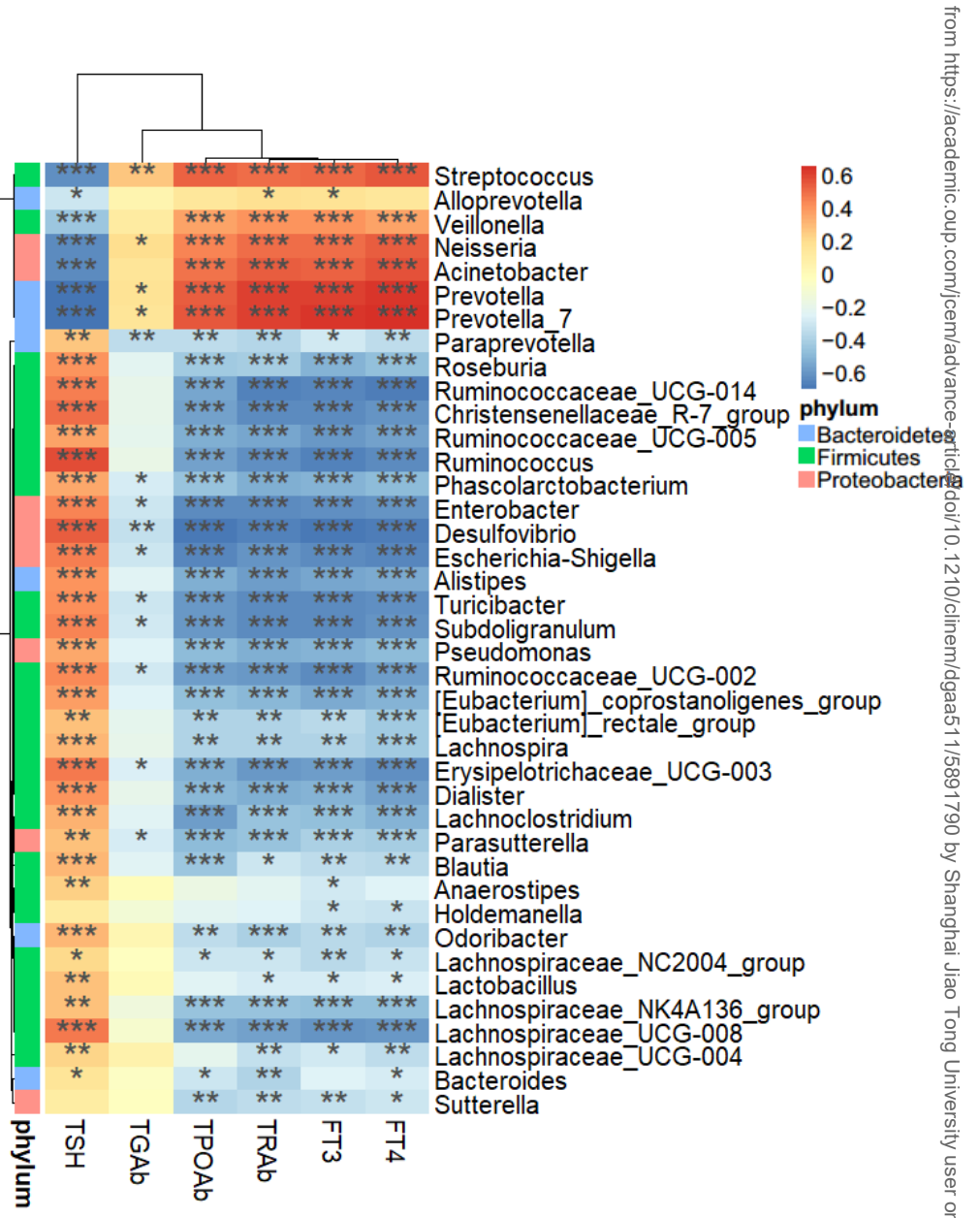

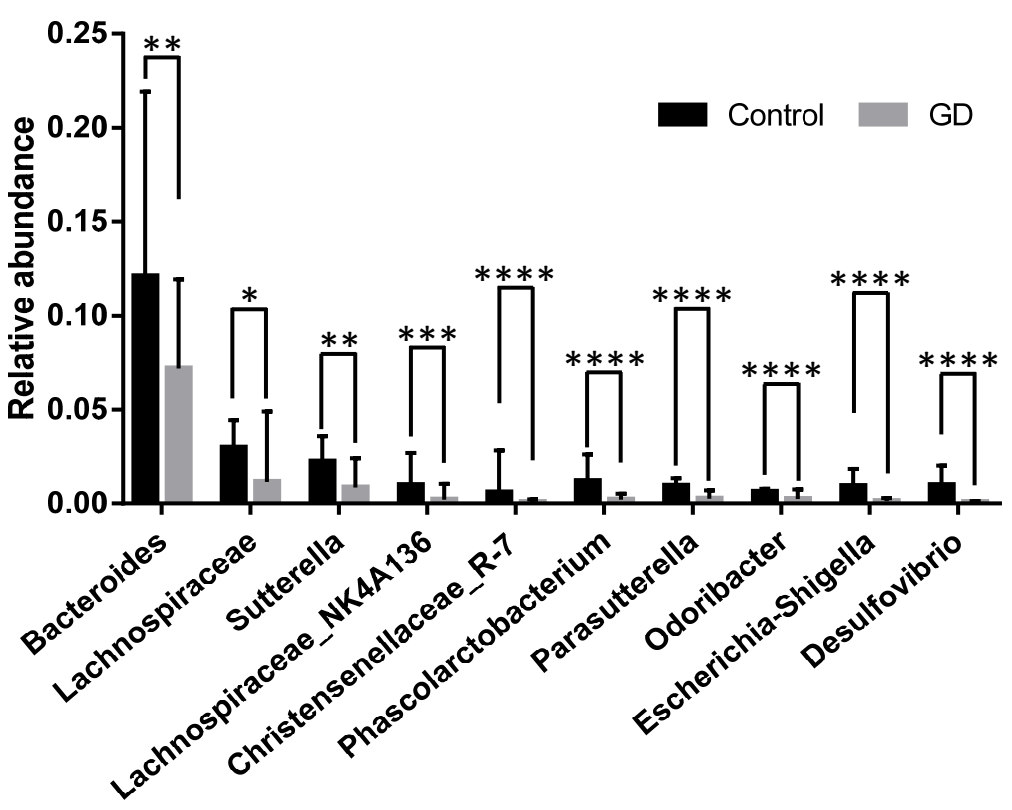

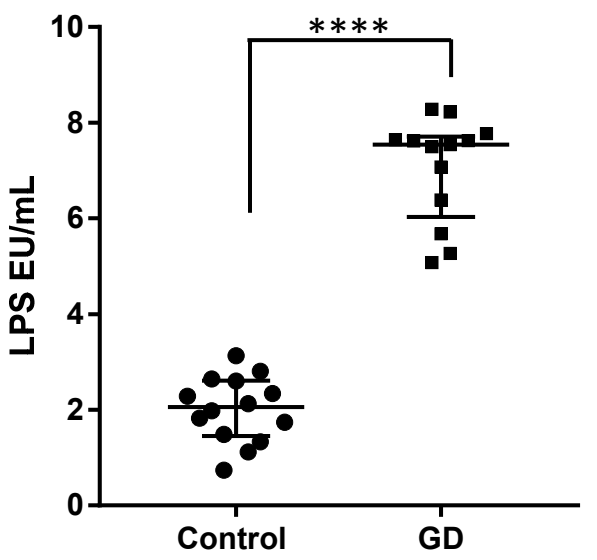

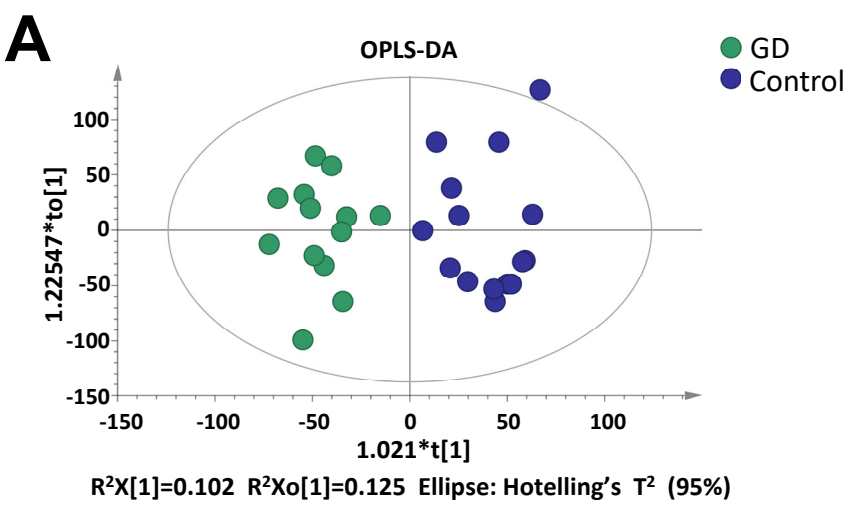

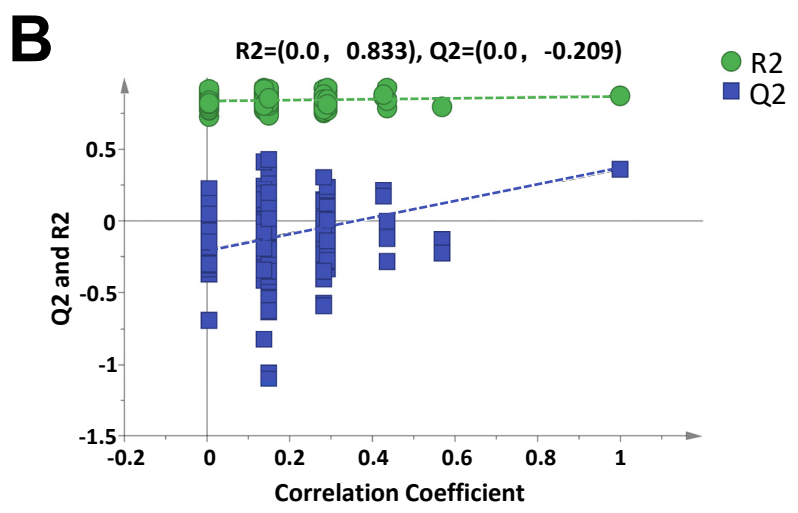

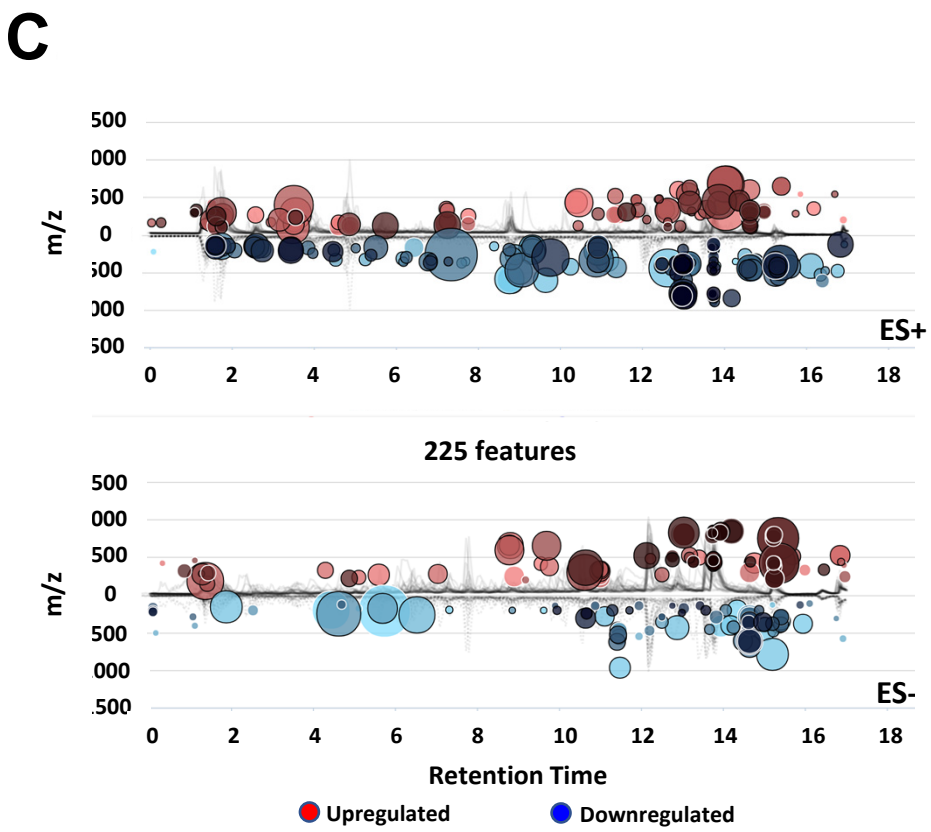

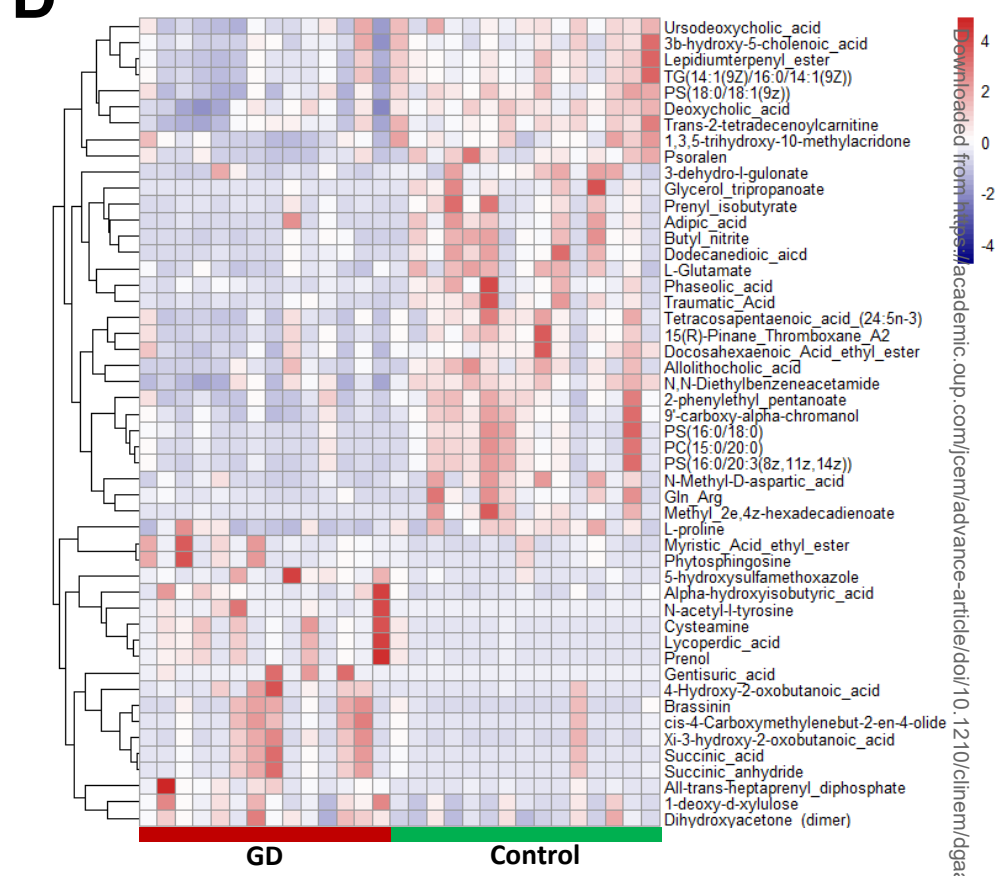

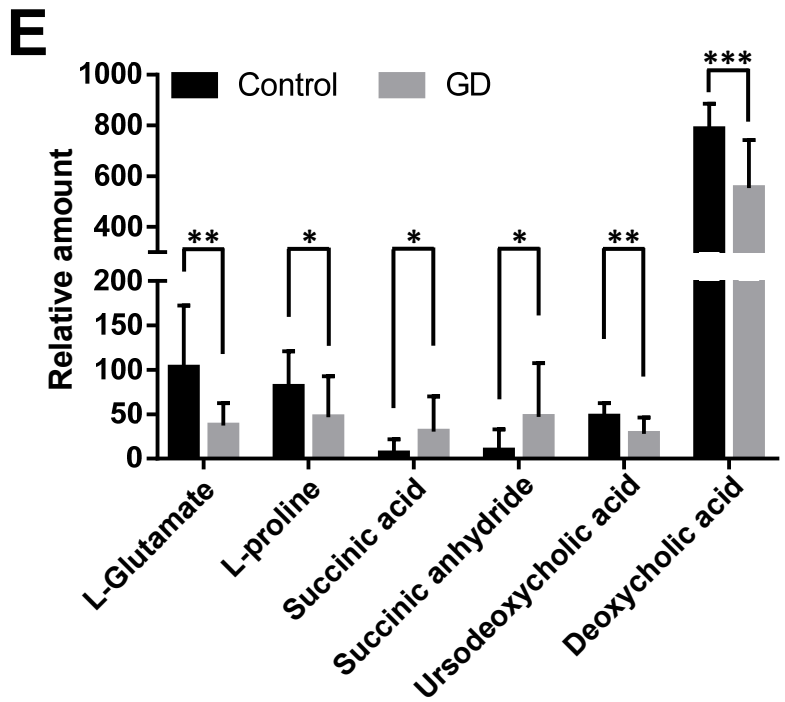

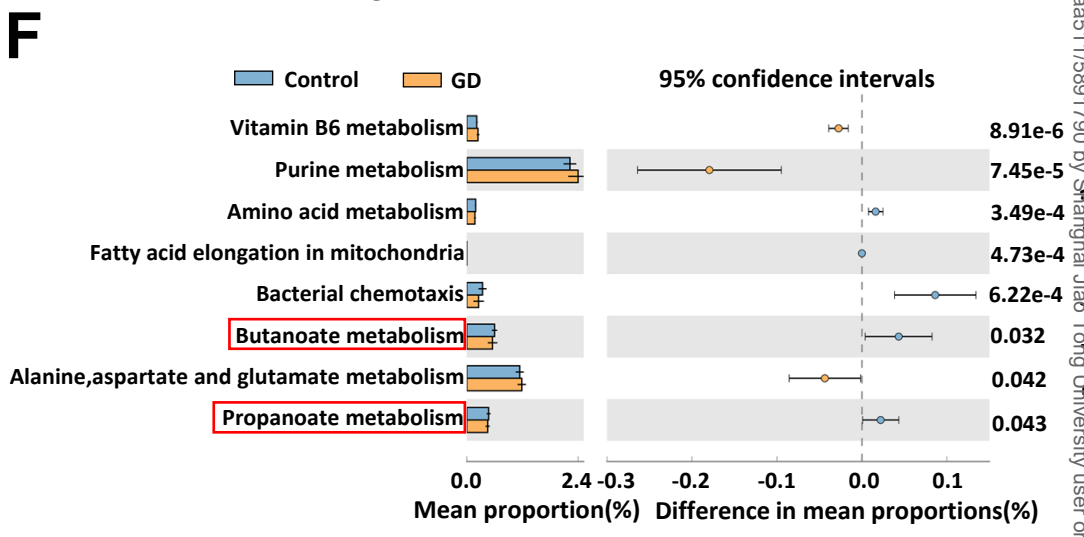

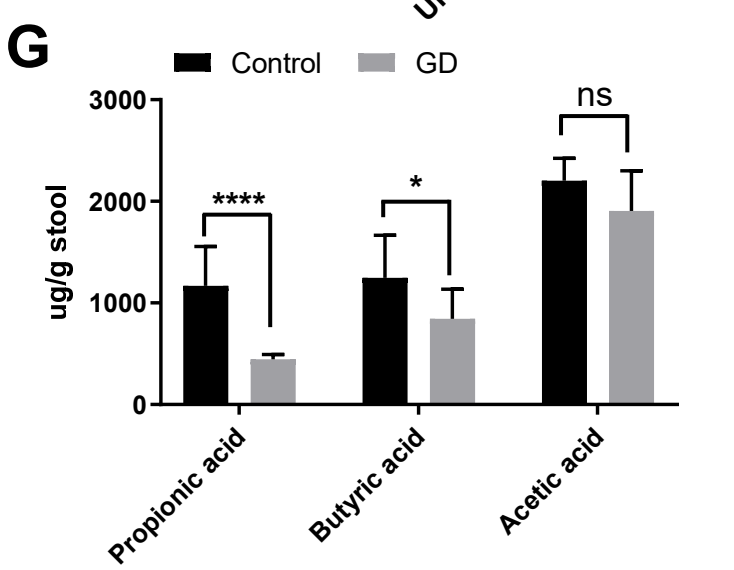

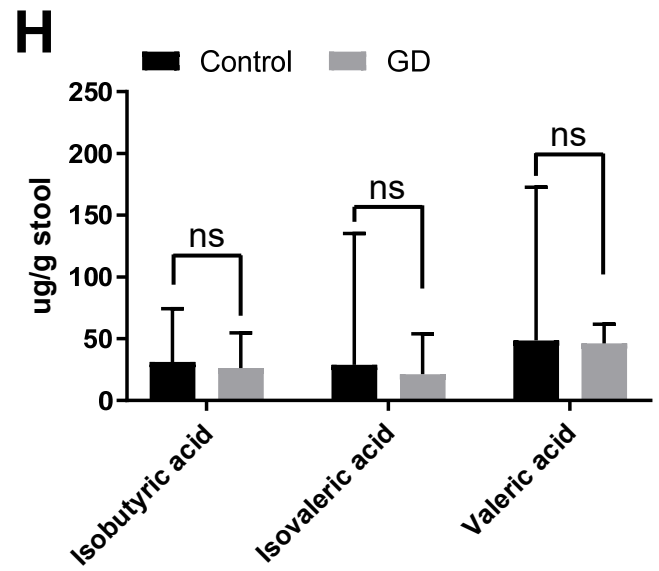

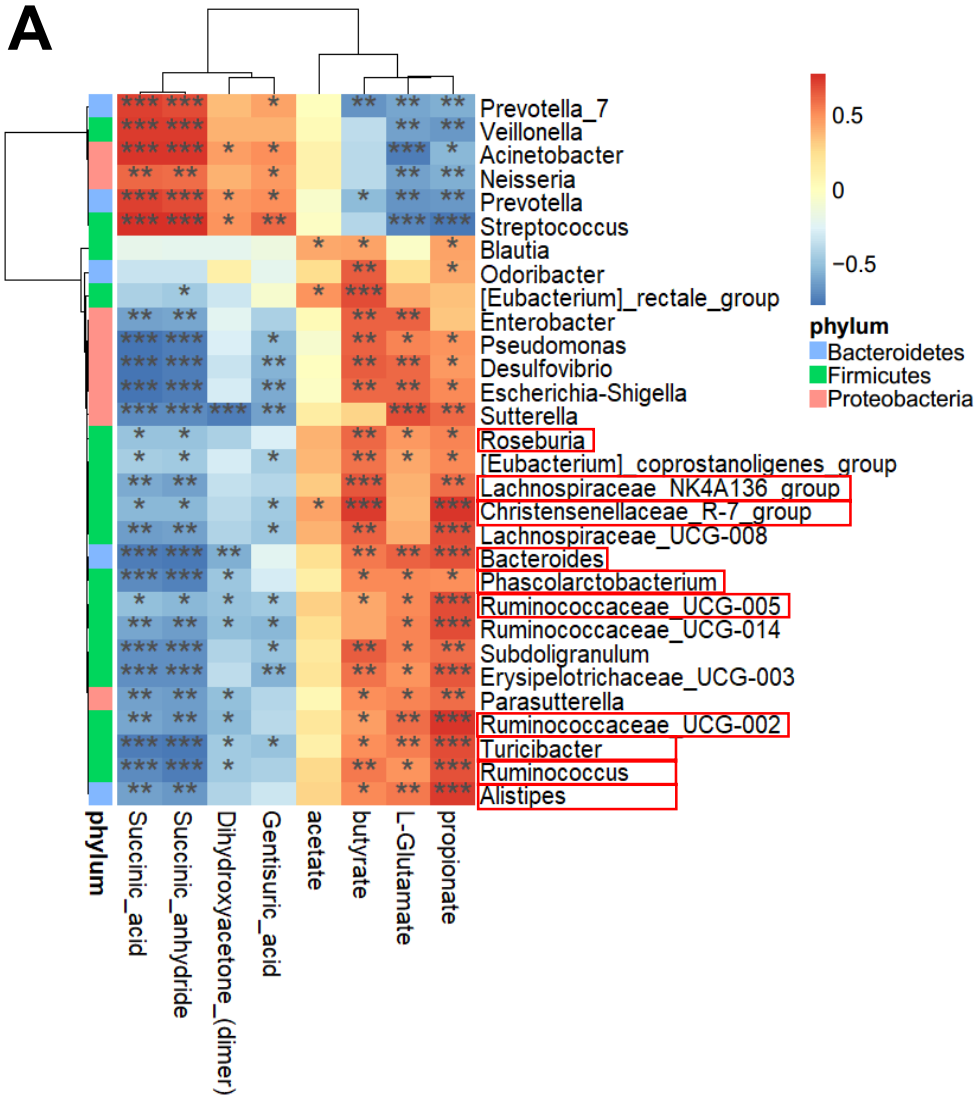

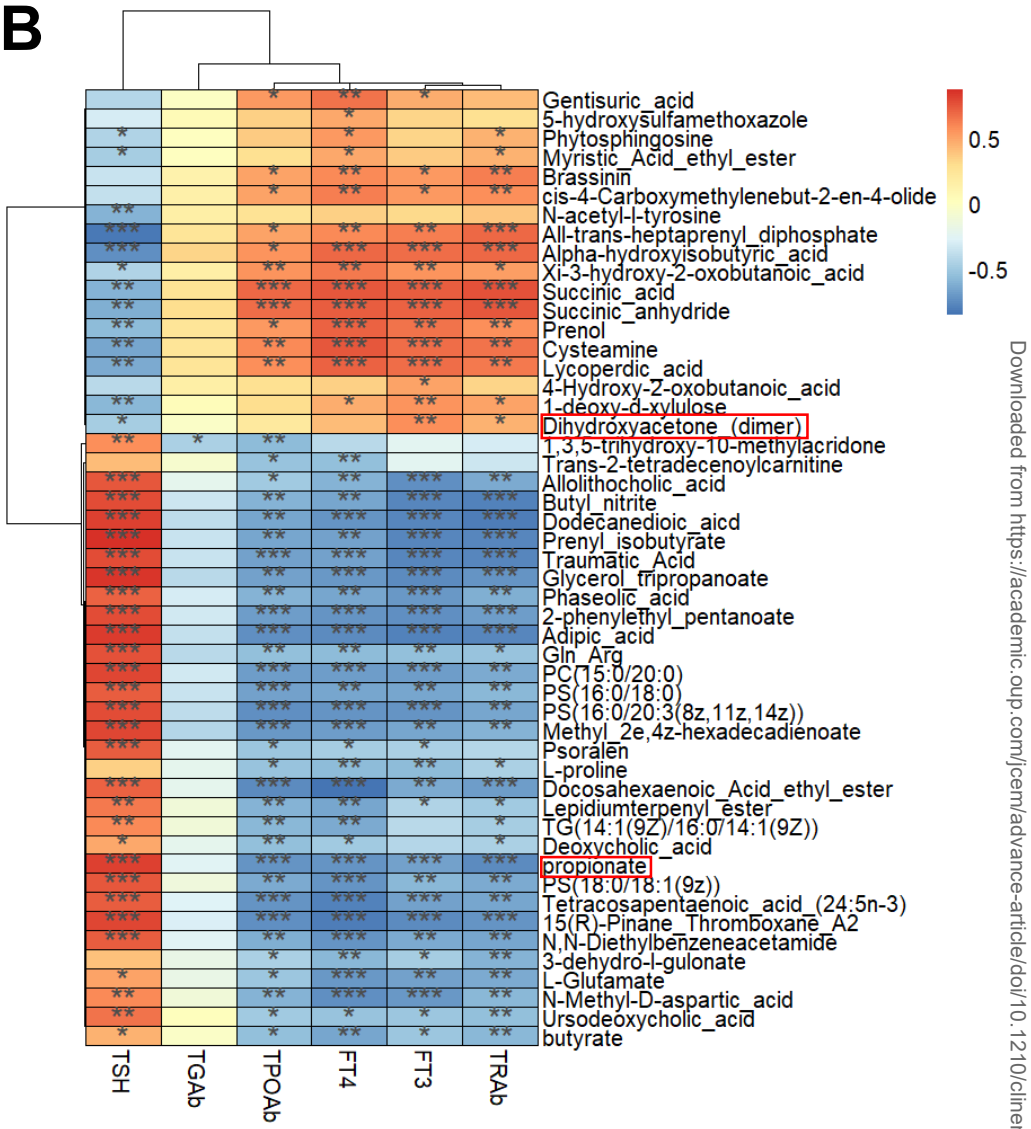

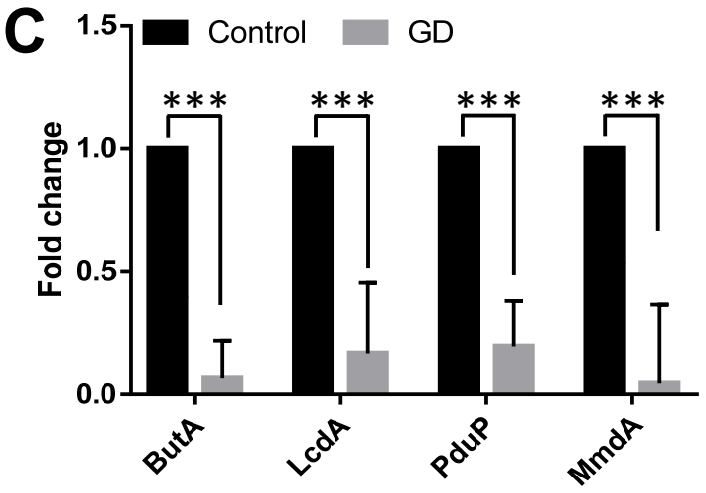

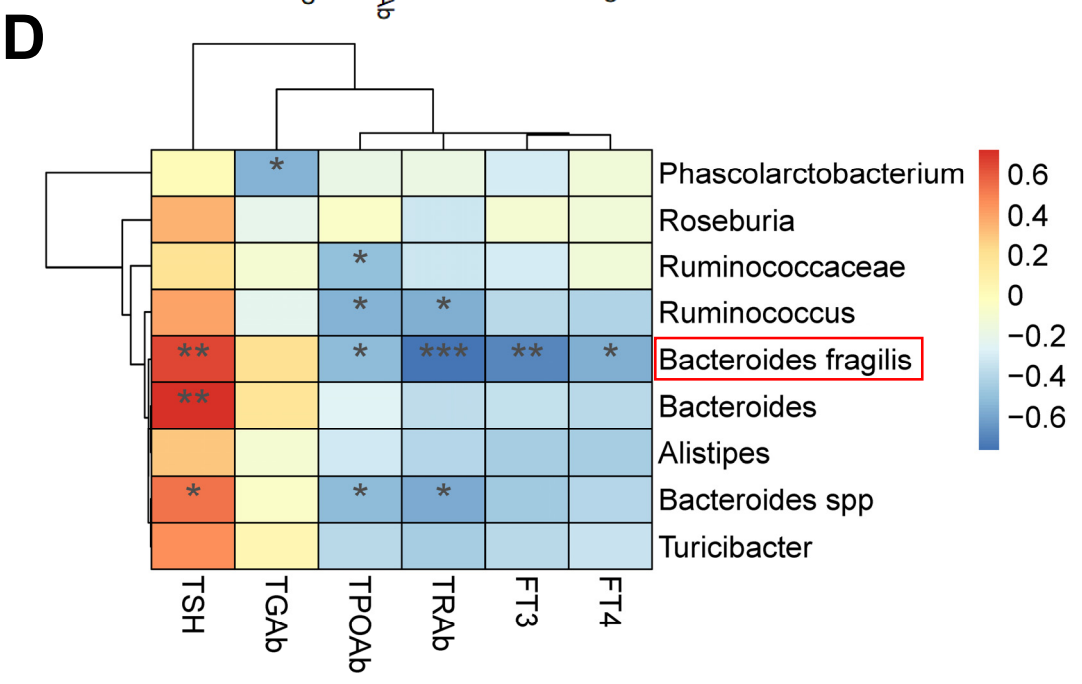

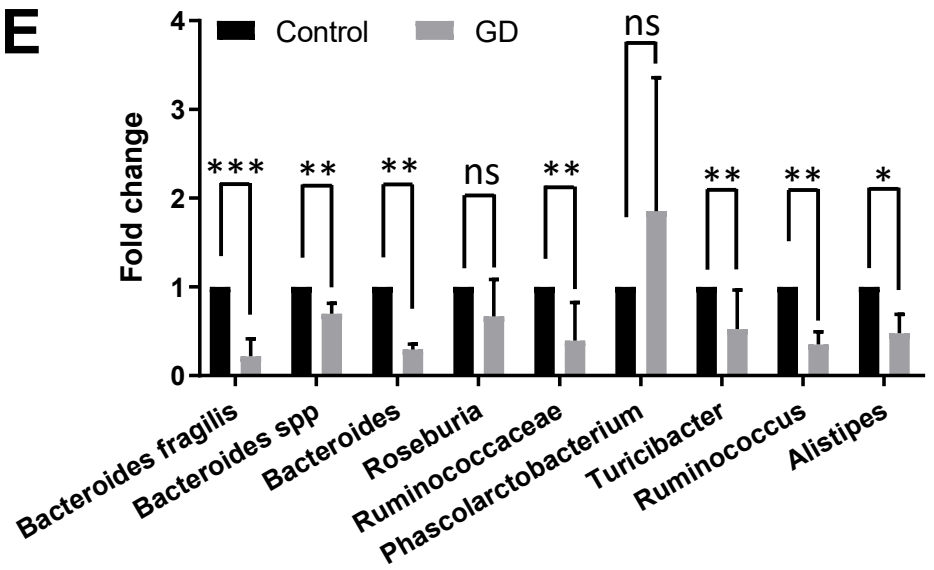

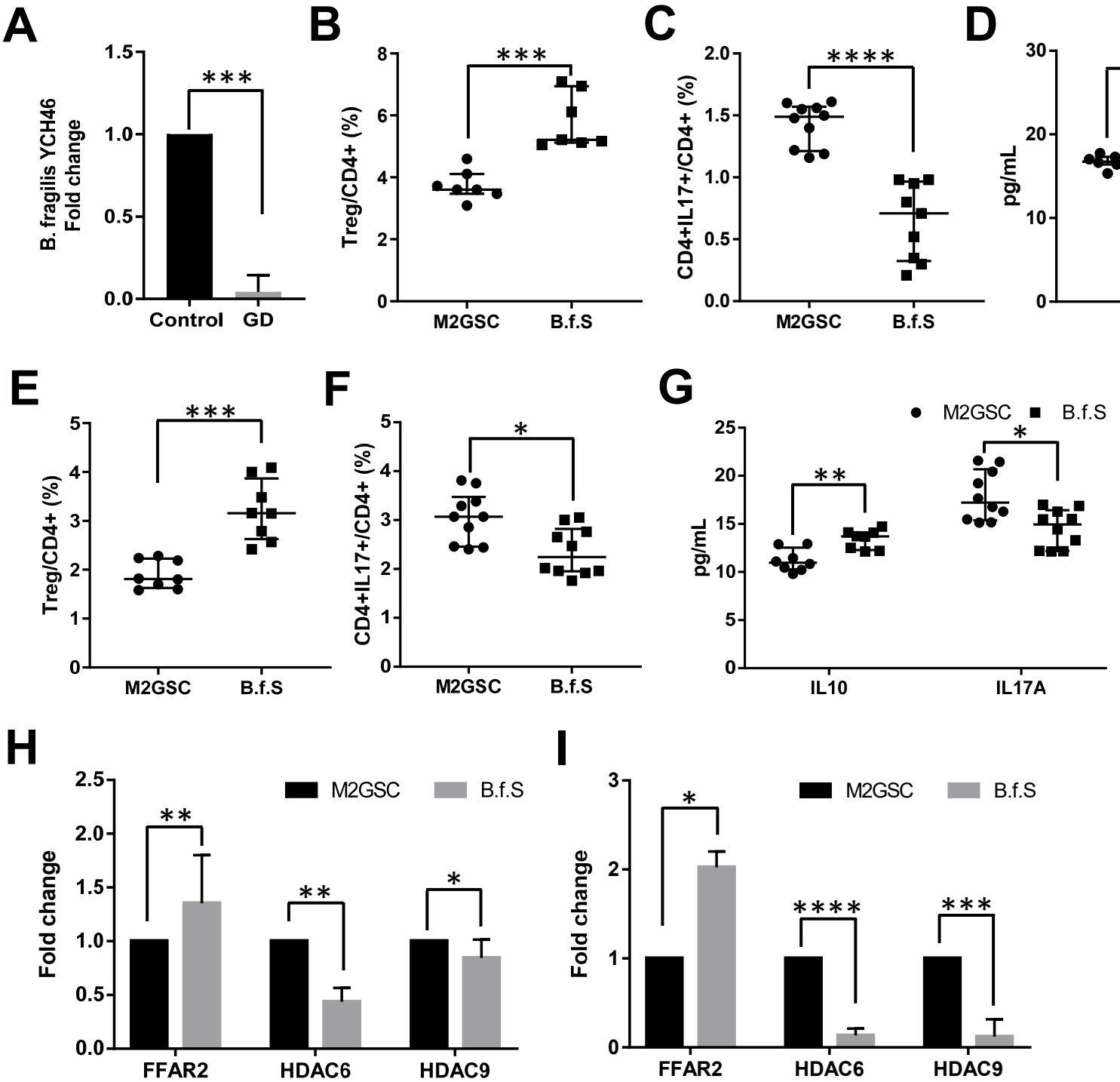

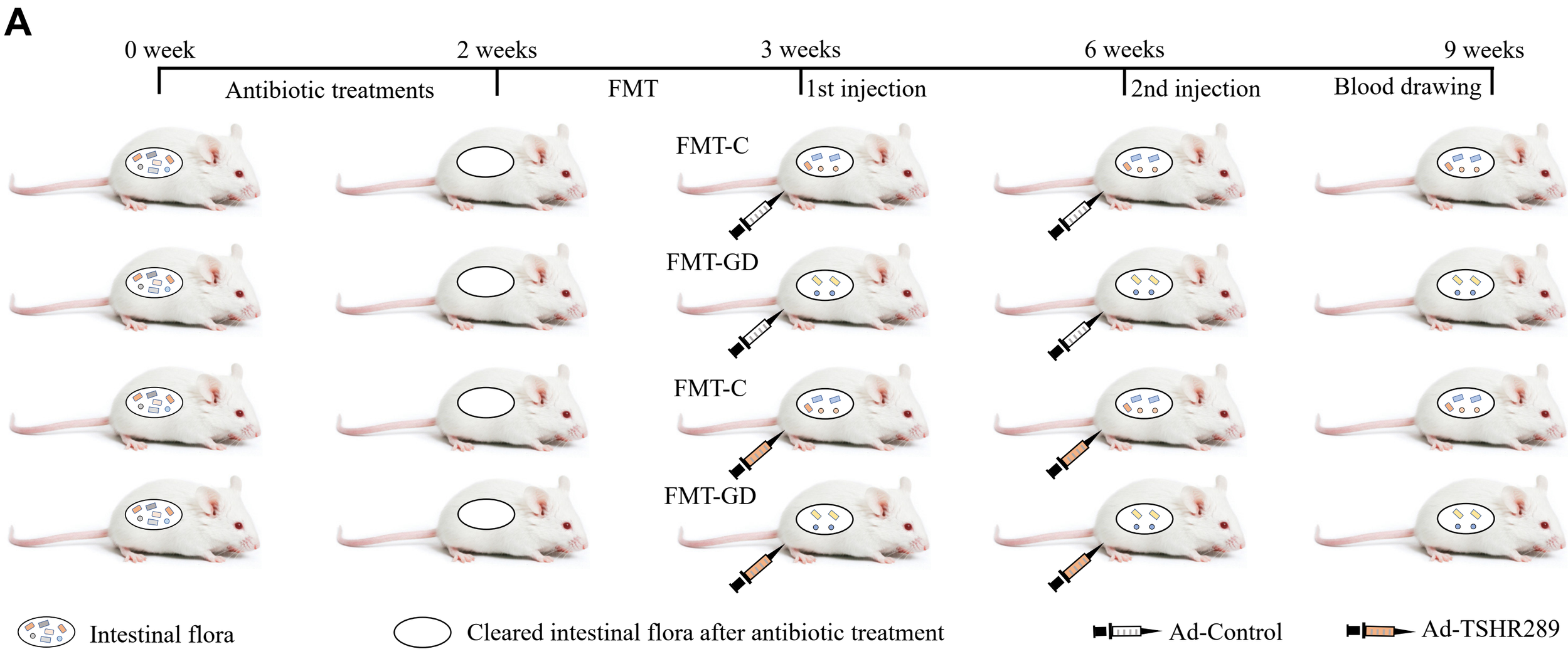

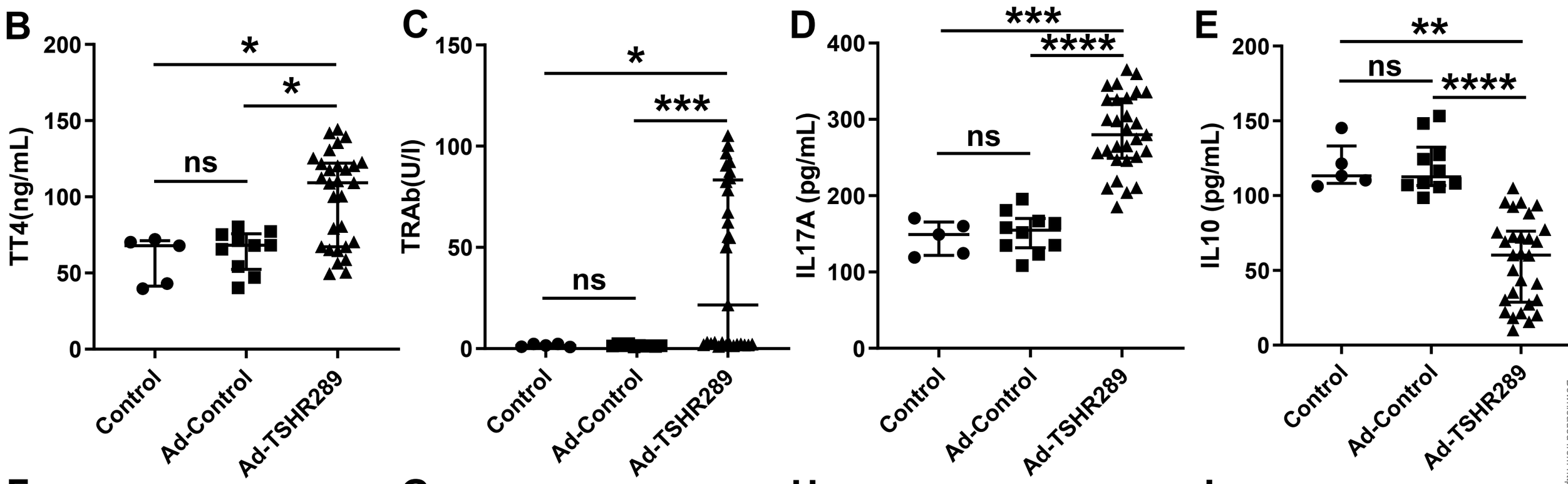

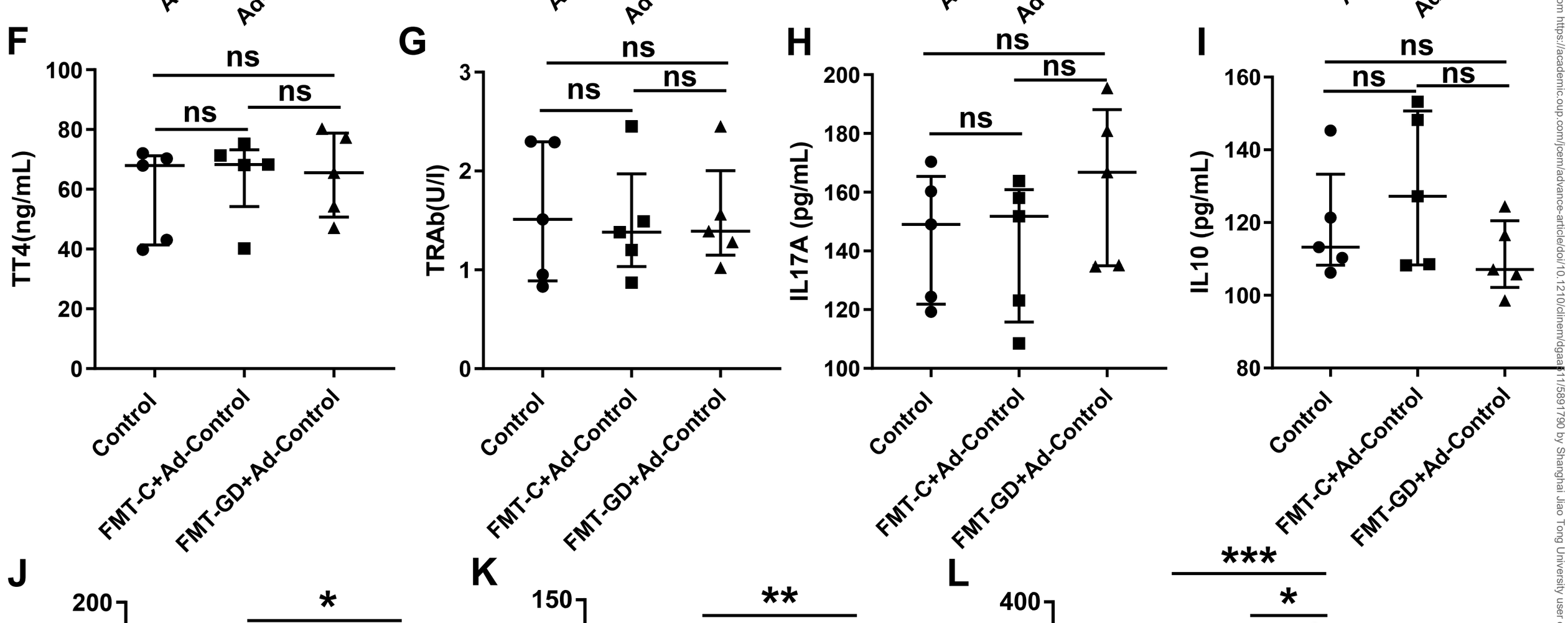

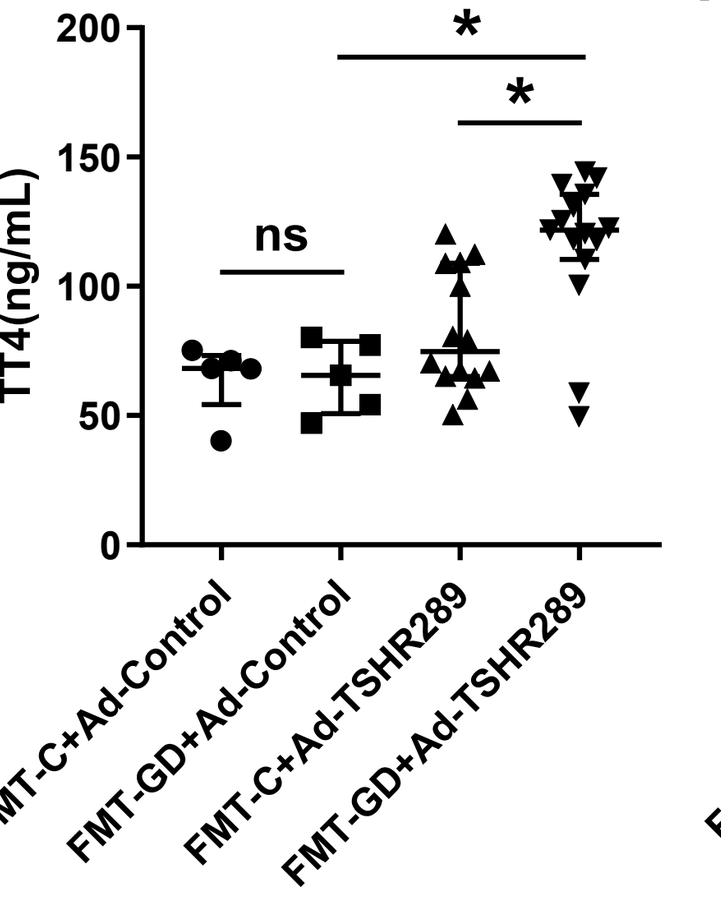

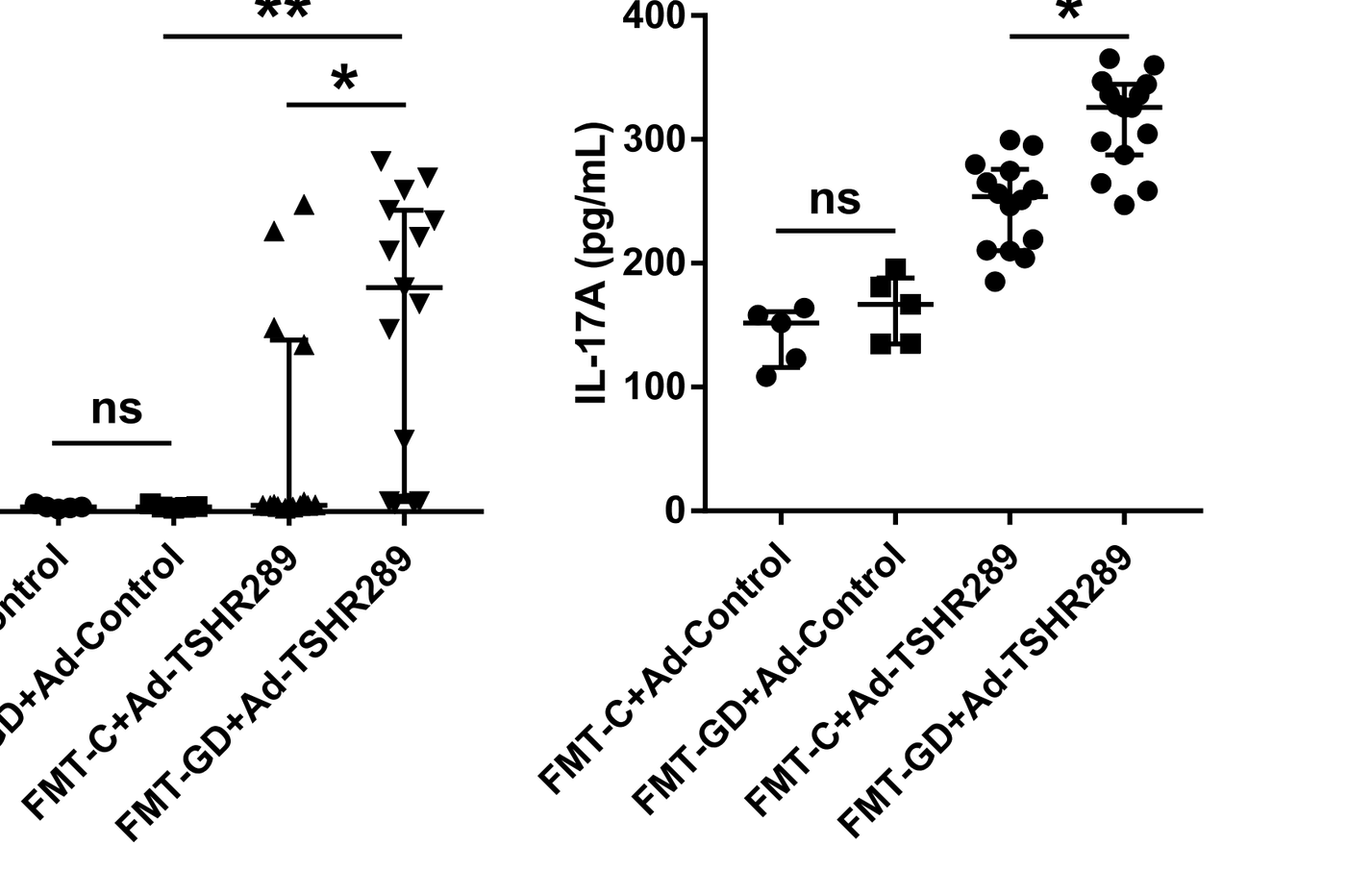

Bacteroides fragilis

Other SCFAs-producing bacteria

G- bacteria

Butyrate

Propionate

LPS

Gut barrier damage

Lumen

Epithelial cells

GPR43

T cells

HDAC inhibition

Treg

Th17

IL10

IL17

Treg/Th17 Imbalance

Inflammation

LPS

Genetic predisposition

Smoking & Alcohol

Female gender

Pregnancy

Diet

Stress

Infections

Th2

Th1

Bystander activation

Epitope spreading

Loss of Immune Tolerance

B cells

Graves' Disease

TSAb

Molecular mimicry

LPS: Lipopolysaccharides

G-: Gram negative

SCFAs: Short-chain fatty acids